

# A<sup>3</sup>: an Analytical Low-Rank Approximation Framework for Attention

Jeffrey T. H. Wong<sup>\*</sup> Cheng Zhang<sup>\*</sup> Xinye Cao Pedro Gimenes

George A. Constantinides Wayne Luk Yiren Zhao

Department of Electrical and Electronic Engineering

Imperial College London

{tsz.wong20, cheng.zhang122, xinye.cao22, pedro.gimenes19}@imperial.ac.uk

{g.constantinides, w.luk, a.zhao}@imperial.ac.uk

## Abstract

Large language models have demonstrated remarkable performance; however, their massive parameter counts make deployment highly expensive. Low-rank approximation offers a promising compression solution, yet existing approaches have two main limitations: (1) They focus on minimizing the output error of individual linear layers, without considering the architectural characteristics of Transformers, and (2) they decompose a large weight matrix into two small low-rank matrices. Consequently, these methods often fall short compared to other compression techniques like pruning and quantization, and introduce runtime overhead such as the extra GEMM kernel launches and memory operations for decomposed small matrices. To address these limitations, we propose A<sup>3</sup>, a post-training low-rank approximation framework. A<sup>3</sup> splits a Transformer layer into three functional components, namely QK, OV, and MLP. For each component, A<sup>3</sup> provides an analytical solution that reduces the hidden dimension size inside each component while minimizing the component’s functional loss (*i.e.*, error in attention scores, attention outputs, and MLP outputs). This approach directly reduces model sizes, KV cache sizes, and FLOPs without introducing any runtime overheads. In addition, it provides a new narrative in advancing the optimization problem from singular linear layer loss optimization toward improved end-to-end performance. Through extensive experiments, we show that A<sup>3</sup> maintains superior performance compared to SoTAs. For example, under the same reduction budget in computation and memory, our low-rank approximated LLaMA 3.1-70B achieves a perplexity of 4.69 on WikiText-2, outperforming the previous SoTA’s 7.87 by 3.18. We also show versatile applications of A<sup>3</sup>, including its use in KV cache compression, integration with quantization, and mixed-rank assignments for further performance improvements.

## 1 Introduction

Large language models (LLMs) have shown exceptional performance in various applications, including language understanding, code completion, and reasoning tasks [Vaswani et al., 2017, Brown et al., 2020, Chen et al., 2021a, Wei et al., 2022]. However, these models usually contain billions of parameters, resulting in high computational costs and memory requirements. Linear layers and the attention mechanism contribute significantly to the model size and computational complexity, while the KV cache produced during generation further exacerbates the memory burden.

<sup>1</sup>Shared first authorship. Alphabetical by last name.

Low-rank approximation is a promising technique that breaks down a matrix into smaller sub-matrices, directly reducing computational complexity and memory usage without the need of additional specialized hardware support. Usually a trained linear layer  $\mathbf{W} \in \mathbb{R}^{m \times n}$  is approximated by  $\mathbf{W}_r = \mathbf{A}_r \mathbf{B}_r$ , where  $\mathbf{A}_r \in \mathbb{R}^{m \times r}$  and  $\mathbf{B}_r \in \mathbb{R}^{r \times n}$  are two rank- $r$  matrices with  $r \ll m, n$ . At inference time, the original GEMM operation  $\mathbf{XW}$  is replaced by two smaller GEMM operations  $\mathbf{XA}_r$  and  $(\mathbf{XA}_r)\mathbf{B}_r$ . The challenge is to construct the optimal  $\mathbf{A}_r$  and  $\mathbf{B}_r$  that maintains the end-to-end model performance. Recent studies show that minimizing the layer output error instead of the weight error gives better model performance [Zhang et al., 2024a,b], thus various activation-aware methods have been proposed, such as SVD-LLM [Wang et al., 2024], ASVD [Yuan et al., 2023], FWSVD [Hsu et al., 2022]. However, these methods usually target general linear layers, which save FLOPs and memory proportional to  $\frac{m+n}{mn}r$  (Note that  $\frac{m+n}{mn}r < r$  for any  $m, n > 2$ ). Moreover, these methods rarely consider the architectural characteristics of Transformer, and suffer from severe performance degradation when compared to pruning and quantization.

To address these limitations, we propose  $\mathbf{A}^3$ , a new analytical framework for post-training low-rank approximation.  $\mathbf{A}^3$  splits the Transformer architecture into three functional components: query-key (QK) component, output-value (OV) component, and multi-layer perceptron (MLP) component, and minimizes the functional loss of each component. This three-part decomposition is inspired by the mechanistic interoperability of the Transformer architecture [Elhage et al., 2021], allowing a close alignment of local optimization goals with the overall end-to-end model performance.

We highlight the following contributions of  $\mathbf{A}^3$ :

- We propose a three-part low-rank approximation setup for multi-head attention (MHA), which formulates the problem as three separate objectives: minimizing the functional loss of (1) QK’s attention score, (2) OV’s attention output, and (3) MLP’s layer output.
- We derive closed-form solutions for the three objectives, which reduces the hidden dimensions shared within each component: QK head dimension, OV head dimension, and MLP intermediate size. This naturally reduces model sizes, KV cache sizes, FLOPs, and avoids runtime overheads like extra GEMM operations. Moreover,  $\mathbf{A}^3$  trims both FLOPs/memory and information energy proportionally to the rank  $r$ , enabling a more effective trade-off between model performance and hardware efficiency.
- We have adapted  $\mathbf{A}^3$  for use with diverse Transformer architectures, including group query attention (GQA) and rotary position embedding (RoPE), which allows the application of  $\mathbf{A}^3$  across a broad spectrum of models. This overcomes the limitation of existing low-rank approximation methods, which can only be applied on the vanilla MHA architecture.
- We conduct extensive experiments on various LLMs, and show that  $\mathbf{A}^3$  outperforms SoTA low-rank methods by a significant margin. For example, our compressed LLaMA 3.1-70B achieves a perplexity of 4.69 on WikiText-2, outperforming SoTA method’s 7.87 by 3.18. We also demonstrate further applications of  $\mathbf{A}^3$ , such as its effectiveness in KV cache reduction, combination with quantization, and mixed-rank assignments for better performance.

## 2 Related Work

**Transformer and its variants** The attention layer and the multi-layer perceptron layer (MLP) are two main modules of the Transformer architecture. In vanilla multi-head attention (MHA) [Vaswani et al., 2017], QK component computes the attention scores as follows:

$$\mathbf{A}'_i = \text{row\_softmax}(\mathbf{A}_i / \sqrt{d_{\text{qk}}}) = \text{row\_softmax}(\mathbf{Q}_i \mathbf{K}_i^T / \sqrt{d_{\text{qk}}}) . \quad (1)$$

where  $\mathbf{A}_i$  is the pre-softmax attention score of  $i$ -th head, and  $d_{\text{qk}}$  is the head dimension shared by  $\mathbf{Q}_i$  and  $\mathbf{K}_i$ . The post-softmax attention score is then multiplied with the value and summed over all heads to form the attention output:

$$\mathbf{O} = \sum_i^{h_q} \mathbf{A}'_i \mathbf{V}_i \mathbf{W}_{o,i} . \quad (2)$$

Note that there is a head dimension  $d_{\text{vo}}$  shared by  $\mathbf{V}_i$  and  $\mathbf{W}_{o,i}$ . In practice,  $\mathbf{W}_{o,i}$  are usually concatenated as a single linear layer,  $\mathbf{W}_o = [\mathbf{W}_{o,1}^T, \mathbf{W}_{o,2}^T, \dots, \mathbf{W}_{o,h_q}^T]^T$ .

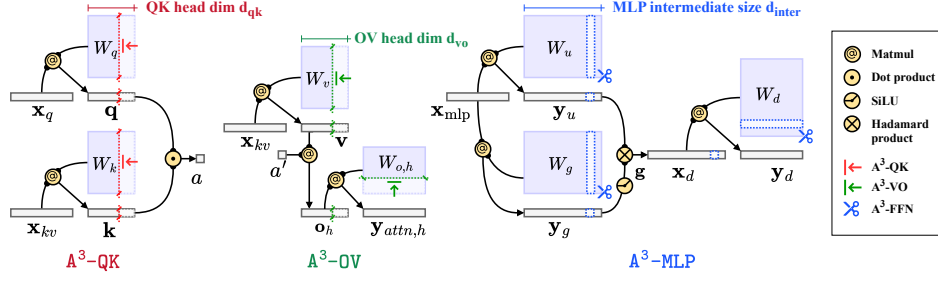


Figure 1: High-level overview of  $A^3$ .  $A^3$  performs a low-rank approximation on each QK, OV, and MLP component, reducing the head dimensions in QK and OV, and the intermediate dimension in MLP.

The classic MLP in a Transformer has two linear layers with a ReLU activation function in between:

$$X_d = \text{ReLU}(X_{\text{mlp}} W_u), \quad Y_{\text{mlp}} = X_d W_d. \quad (3)$$

$W_u$  and  $W_d$  scale the input dimension  $d_m$  to the intermediate dimension  $d_{\text{inter}}$  and back to  $d_m$ .

Following the vanilla MHA, numerous Transformer variants have been proposed [Ainslie et al., 2023, Shazeer, 2019, Liu et al., 2024]. In recent models, the 2-layer MLP is usually replaced with a 3-layer variant [Shazeer, 2020]:

$$Y_g = X_{\text{mlp}} W_g, \quad Y_u = X_{\text{mlp}} W_u, \quad X_d = \text{SiLU}(Y_g) \otimes Y_u, \quad Y_{\text{mlp}} = X_d W_d, \quad (4)$$

where  $\otimes$  denotes element-wise multiplication.  $W_u$  and  $W_g$  upscale the input dimension  $d_m$  to  $d_{\text{inter}}$  and  $W_d$  downscale it back to  $d_m$ . Group query attention (GQA) [Ainslie et al., 2023] is another widely adopted variant sharing a reduced number of key and value heads among groups of query heads. Besides, many LLMs adopt rotary positional embedding (RoPE) [Su et al., 2024].

Inspired by [Elhage et al., 2021], we split the Transformer layer into three key components: QK (Equation (1)), OV (Equation (2)), and MLP (Equation (3)). We highlight that there are three hidden dimensions, the two head dimensions  $d_{\text{qk}}$  and  $d_{\text{vo}}$ , and one MLP intermediate size  $d_{\text{inter}}$ , shared within each component but reduced inside the component, while the inter-Transformer layer dimensions are kept at  $d_m$ . Accordingly, as shown in Figure 1, our method  $A^3$  consists of three parts,  $A^3\text{-QK}$ ,  $A^3\text{-OV}$ , and  $A^3\text{-MLP}$ , to compresses the three hidden dimensions.

**Low-rank approximation for compressing Transformers** The linear layer takes a simple form but contributes most parameters to Transformer. For compressing large Transformer models like LLMs, low-rank approximation has been widely studied [Chen et al., 2021b, Saha et al., 2024]. Usually a trained linear layer  $W \in \mathbb{R}^{m \times n}$  is approximated by  $W \approx \widetilde{W}_r = A_r B_r$ , where  $A_r \in \mathbb{R}^{m \times r}$  and  $B_r \in \mathbb{R}^{r \times n}$  are two rank- $r$  matrices that effectively reduce the number of parameters and FLOPs with a small enough  $r$ . The problem is how to find the optimized  $A_r$  and  $B_r$  that maintains the model performance. If the objective is to minimize the Frobenius (or spectral) norm of the weight error,

$$\text{argmin}_{\widetilde{W}_r} \|W - \widetilde{W}_r\|_F^2 \quad \text{s.t.} \quad \text{rank}(\widetilde{W}_r) = r, \quad (5)$$

according to Eckart-Young theorem [Eckart and Young, 1936a], the optimal solution is to perform truncated singular value decomposition (SVD) on the weight matrix  $W$ .

$$W = U \Sigma V^T, \quad \widetilde{W}_r = \text{SVD}_r(W) = U_{:, :r} \Sigma_{:, :r} V_{:, :r}^T, \quad (6)$$

where  $U \in \mathbb{R}^{m \times k}$  and  $V \in \mathbb{R}^{k \times n}$  are the left and right singular vectors and  $\Sigma \in \mathbb{R}^{k \times k}$  is the diagonal matrix of singular values. Recent studies show that minimizing the layer output error instead of the weight error gives better end-to-end model performance [Zhang et al., 2024a,b],

$$\text{argmin}_{\widetilde{W}_r} \mathbb{E}_{x \sim \mathbb{X}} \|xW - x\widetilde{W}_r\|_2^2 \quad \text{s.t.} \quad \text{rank}(\widetilde{W}_r) = r, \quad (7)$$

where  $x \in \mathbb{R}^d$  denotes the input vector of size  $d$ . The objective above minimizes the expected  $l_2$ -norm of layer output error. Recent studies find the optimal solution is:

$$\widetilde{W}_k = (R_{\mathbb{X}\mathbb{X}}^{\frac{1}{2}})^{-1} \text{SVD}_r(R_{\mathbb{X}\mathbb{X}}^{\frac{1}{2}} W), \quad (8)$$

assuming  $\mathbf{R}_{\mathbb{X}\mathbb{X}}$  is positive definite, where  $\mathbf{R}_{\mathbb{X}\mathbb{X}} = \mathbb{E}_{\mathbf{x} \sim \mathbb{X}} \{\mathbf{x}^T \mathbf{x}\}$  is the autocorrelation matrix with respect to the input space  $\mathbb{X} \subseteq \mathbb{R}^d$ , and  $\mathbf{R}_{\mathbb{X}\mathbb{X}}^{\frac{1}{2}}$  denotes the unique symmetric square root of  $\mathbf{R}_{\mathbb{X}\mathbb{X}}$ .

Interestingly, there are several works proposing or leveraging the solution in Equation (8) for various applications. DRONE [Chen et al., 2021b] and SVD-LLM [Wang et al., 2024] directly apply the solution to approximate all linear layers in Transformers. QERA [Zhang et al., 2024b] uses it to build high-precision low-rank terms to compensate for output quantization error, while CALDERA [Saha et al., 2024] further proposes iterative methods to quantize the low-rank terms, achieving performant sub-2.5-bit post-training quantization. Palu [Chang et al., 2024] reduces KV cache size by decomposing key and value weight matrices with the solution and caching smaller intermediate activations instead of original keys and values.

However, these works target general linear layers and minimize the linear layer output error without considering architectural characteristics. In this work, we step forward to the optimization for functional components. We propose analytical low-rank approximation methods of compressing the QK, OV, and MLP components that minimize the functional errors of attention scores, attention outputs, and MLP outputs, respectively.

### 3 The A<sup>3</sup> Framework

In this section, for each component (QK, OV, MLP), we define the problem (optimization objectives), clarify the assumptions if any, and propose our analytical solutions. The proof for each lemma and theorem is provided in the Appendix. We also provide notation tables in Tables 3 and 4 in the appendix for the ease of reading.

#### 3.1 A<sup>3</sup>-QK

In the QK component, each head computes its pre-softmax attention scores between queries and keys:

$$a_i = \mathbf{q}_i \mathbf{k}_i^T = \mathbf{x}_q \mathbf{W}_{q,i} \mathbf{W}_{k,i}^T \mathbf{x}_{kv}^T = \mathbf{x}_q \mathbf{W}_{qk,i} \mathbf{x}_{kv}^T, \quad (9)$$

where  $\mathbf{x}_q, \mathbf{x}_{kv} \in \mathbb{R}^{d_m}$  are the input vectors of query layer and key/value layer respectively, and  $\mathbf{W}_{qk,i} := \mathbf{W}_{q,i} \mathbf{W}_{k,i}^T$  denotes the fused weight matrix of the  $i$ -th head. We seek for the low-rank approximation of  $\mathbf{W}_{qk,i}$  that minimizes the error of pre-softmax attention scores.

**Problem 1** (Minimization of the pre-softmax attention score error). Given a pretrained Transformer layer, for the  $i$ -th head of QK component  $a_i = \mathbf{x}_q \mathbf{W}_{qk,i} \mathbf{x}_{kv}^T$  and its rank- $r$  approximated form  $\tilde{a}_i = \mathbf{x}_q \tilde{\mathbf{W}}_{qk,i} \mathbf{x}_{kv}^T$ , approximating the head by minimizing the error between  $a_i$  and  $\tilde{a}_i$  is to minimize the following expectation.

$$\operatorname{argmin}_{\tilde{\mathbf{W}}_{qk,i}} \mathbb{E}_{\mathbf{x}_q \sim \mathbb{X}_q, \mathbf{x}_{kv} \sim \mathbb{X}_{kv}} \{(\mathbf{x}_q (\mathbf{W}_{qk,i} - \tilde{\mathbf{W}}_{qk,i}) \mathbf{x}_{kv}^T)^2\} \quad \text{s.t.} \quad \operatorname{rank}(\tilde{\mathbf{W}}_{qk,i}) = r, \quad (10)$$

where  $\mathbb{X}_q \subseteq \mathbb{R}^{d_m}$  and  $\mathbb{X}_{kv} \subseteq \mathbb{R}^{d_m}$  are the input spaces for query and key/value. In practice, the expectation can be approximated as a sample mean on a small calibration dataset.

**Lemma 1** (Equivalent form of Problem 1). *Under the assumption that  $\mathbf{x}_q \sim \mathbb{X}_q$  and  $\mathbf{x}_{kv} \sim \mathbb{X}_{kv}$  are independent, the objective in Problem 1 is equivalent to:*

$$\operatorname{argmin}_{\tilde{\mathbf{W}}_{qk,i}} \|\mathbf{R}_{\mathbb{X}_q \mathbb{X}_q}^{\frac{1}{2}} (\mathbf{W}_{qk,i} - \tilde{\mathbf{W}}_{qk,i}) \mathbf{R}_{\mathbb{X}_{kv} \mathbb{X}_{kv}}^{\frac{1}{2}}\|_F^2, \quad (11)$$

where  $\mathbf{R}_{\mathbb{X}_q \mathbb{X}_q} := \mathbb{E}_{\mathbf{x}_q \sim \mathbb{X}_q} \{\mathbf{x}_q^T \mathbf{x}_q\}$  and  $\mathbf{R}_{\mathbb{X}_{kv} \mathbb{X}_{kv}} := \mathbb{E}_{\mathbf{x}_{kv} \sim \mathbb{X}_{kv}} \{\mathbf{x}_{kv}^T \mathbf{x}_{kv}\}$  are the autocorrelation matrices of the input spaces  $\mathbb{X}_q$  and  $\mathbb{X}_{kv}$  respectively.  $\mathbf{R}_{\mathbb{X}_q \mathbb{X}_q}^{\frac{1}{2}}$  and  $\mathbf{R}_{\mathbb{X}_{kv} \mathbb{X}_{kv}}^{\frac{1}{2}}$  denote the corresponding unique symmetric matrix square roots.

The assumption discussion and the complete derivation of Lemma 1 are provided in Appendices B.1.1 and B.1.2.

**Theorem 2** (A<sup>3</sup>-QK for MHA-NoPE). *The optimal solution to Problem 1 is*

$$\tilde{\mathbf{W}}_{qk,i} = \left(\mathbf{R}_{\mathbb{X}_q \mathbb{X}_q}^{\frac{1}{2}}\right)^{-1} \operatorname{SVD}_r \left(\mathbf{R}_{\mathbb{X}_q \mathbb{X}_q}^{\frac{1}{2}} \mathbf{W}_{qk,i} \mathbf{R}_{\mathbb{X}_{kv} \mathbb{X}_{kv}}^{\frac{1}{2}}\right) \left(\mathbf{R}_{\mathbb{X}_{kv} \mathbb{X}_{kv}}^{\frac{1}{2}}\right)^{-1}, \quad (12)$$

where  $\operatorname{SVD}_r(\cdot)$  denotes the truncated SVD operator.

The proof of Theorem 2 is given in Appendix B.1.3. In practice, we apply Theorem 2 to all pairs of QK heads ( $i = 1, \dots, h_q$ ), and assign

$$\widetilde{\mathbf{W}}_{q,i} := \left( \mathbf{R}_{\mathbb{X}_q \mathbb{X}_q}^{\frac{1}{2}} \right)^{-1} \mathbf{U}_{:,k}, \quad \widetilde{\mathbf{W}}_{k,i}^T := \boldsymbol{\Sigma}_{:,k,:k} \mathbf{V}_{:,k,:}^T \left( \mathbf{R}_{\mathbb{X}_{kv} \mathbb{X}_{kv}}^{\frac{1}{2}} \right)^{-1}, \quad (13)$$

where  $\mathbf{U}_{:,k}$ ,  $\boldsymbol{\Sigma}_{:,k,:k}$ , and  $\mathbf{V}_{:,k,:}^T$  are the truncated SVD components given by Theorem 2. This gives approximated query and key weights with a new smaller head dimension  $r < d_{qk}$ . Note that though Theorem 2 is performed on each head separately, the low-rank head weights can still be concatenated together and implemented as a single linear layer.

### 3.2 A<sup>3</sup>-OV

Expand the summation over all OV head outputs in Equation (2). The vector form of the attention layer output  $\mathbf{o} \in \mathbb{R}^{d_m}$  can be expressed as

$$\mathbf{o} = \sum_{i=1}^{h_q} \mathbf{o}_i = \sum_{i=1}^{h_q} a'_i \mathbf{x}_{kv} \mathbf{W}_{v,i} \mathbf{W}_{oi} = \sum_{i=1}^{h_q} \mathbf{p}_i \mathbf{W}_{vo,i}, \quad (14)$$

where  $\mathbf{p}_i := a'_i \mathbf{x}_{kv} \in \mathbb{R}^{d_m}$  is the product between post-softmax attention score and the input vector of key/value layer, and  $\mathbf{W}_{vo,i} := \mathbf{W}_{v,i} \mathbf{W}_{oi} \in \mathbb{R}^{d_m \times d_m}$  denotes the fused weight matrix of the  $i$ -th head. Now each term  $\mathbf{o}_i$  takes the form of a linear layer  $\mathbf{o}_i = \mathbf{p}_i \mathbf{W}_{vo,i}$ . If  $\widetilde{\mathbf{o}}_i = \mathbf{p}_i \widetilde{\mathbf{W}}_{vo,i}$  denotes the approximated  $\mathbf{o}_i$ , the upper bound of the attention output error can be derived as follows:

$$\|\mathbf{o} - \widetilde{\mathbf{o}}\|_2^2 = \left\| \sum_{i=1}^{h_q} (\mathbf{o}_i - \widetilde{\mathbf{o}}_i) \right\|_2^2 \leq \sum_{i=1}^{h_q} \|\mathbf{o}_i - \widetilde{\mathbf{o}}_i\|_2^2. \quad (15)$$

Though  $\|\mathbf{o} - \widetilde{\mathbf{o}}\|_2^2$  can be directly minimized via matrix stacking and truncated SVD, its closed-form solution incurs a higher computational cost, as elaborated in Appendix B.2.3. Here, we treat minimizing each error term  $\|\mathbf{o}_i - \widetilde{\mathbf{o}}_i\|_2^2$  as an independent problem. Thus the optimal solution to  $\widetilde{\mathbf{W}}_{vo,i}$  is already given by Equation (8).

**Problem 2** (Minimization of per-head attention output error). Given a pretrained Transformer layer, for the  $i$ -th head of OV component  $\mathbf{o}_i = \mathbf{p}_i \mathbf{W}_{vo,i}$  and its approximated form  $\widetilde{\mathbf{o}}_i = \mathbf{p}_i \widetilde{\mathbf{W}}_{vo,i}$ , approximating the head by minimizing the head output error is to minimize the following expectation:

$$\operatorname{argmin}_{\widetilde{\mathbf{W}}_{vo,i}} \mathbb{E}_{\mathbf{p}_i \sim \mathbb{P}_i} \{ \|\mathbf{p}_i (\mathbf{W}_{vo,i} - \widetilde{\mathbf{W}}_{vo,i})\|_F^2 \} \quad \text{s.t.} \quad \operatorname{rank}(\widetilde{\mathbf{W}}_{vo,i}) = r. \quad (16)$$

**Theorem 3** (A<sup>3</sup>-OV for MHA-NoPE). *The optimal solution to Problem 2 is*

$$\widetilde{\mathbf{W}}_{vo,i} = \left( \mathbf{R}_{\mathbb{X}_{\mathbf{p}_i} \mathbb{X}_{\mathbf{p}_i}}^{\frac{1}{2}} \right)^{-1} \operatorname{SVD}_r \left( \mathbf{R}_{\mathbb{X}_{\mathbf{p}_i} \mathbb{X}_{\mathbf{p}_i}}^{\frac{1}{2}} \mathbf{W}_{vo,i} \right), \quad (17)$$

where  $\mathbf{R}_{\mathbb{X}_{\mathbf{p}_i} \mathbb{X}_{\mathbf{p}_i}} := \mathbb{E}_{\mathbf{p}_i \sim \mathbb{P}_i}$  is the autocorrelation matrix with respect to the input space of  $\mathbf{p}_i$  and  $\mathbf{R}_{\mathbb{X}_{\mathbf{p}_i} \mathbb{X}_{\mathbf{p}_i}}^{\frac{1}{2}}$  denotes its unique symmetric matrix square root.

Similar to QK component, in practice we assign

$$\widetilde{\mathbf{W}}_{v,i} := \left( \mathbf{R}_{\mathbb{X}_{\mathbf{p}_i} \mathbb{X}_{\mathbf{p}_i}}^{\frac{1}{2}} \right)^{-1} \mathbf{U}_{:,k}, \quad \widetilde{\mathbf{W}}_{vo,i} := \boldsymbol{\Sigma}_{:,k,:k} \mathbf{V}_{:,k,:}^T \left( \mathbf{R}_{\mathbb{X}_{\mathbf{p}_i} \mathbb{X}_{\mathbf{p}_i}}^{\frac{1}{2}} \right)^{-1},$$

to get the approximated value and output weights of head- $i$  with a smaller head dimension  $r < d_{vo}$ .

### 3.3 A<sup>3</sup>-MLP

The non-linear activation function in MLP component prohibits us from directly applying SVD. Instead, we first derive an objective for minimizing the MLP output error, and uses CUR decomposition [Mahoney and Drineas, 2009] to find the low-rank form of MLP weights.

**Problem 3** (Minimization of MLP output error). Given a pretrained down projection layer  $\mathbf{y}_{\text{mlp}} = \mathbf{x}_d \mathbf{W}_d$  in MLP and its approximated low-rank form  $\tilde{\mathbf{y}}_{\text{mlp}} = \tilde{\mathbf{x}}_d \tilde{\mathbf{W}}_d = \mathbf{x}_d \mathbf{U} \mathbf{W}_d$ , minimizing the MLP output error is to minimize the following expectation:

$$\operatorname{argmin}_{\mathbf{U}=\operatorname{diag}(u_1, u_2, \dots, u_{d_{\text{inter}}})} \mathbb{E}_{\mathbf{x}_d \sim \mathbb{X}_d} \{ \|\mathbf{x}_d \mathbf{U} \mathbf{W}_d - \mathbf{x}_d \mathbf{W}_d\|_2^2 \} \quad \text{s.t.} \quad \operatorname{rank}(\mathbf{U}) = r, \quad (18)$$

where  $\mathbf{x}_d \in \mathbb{R}^{d_{\text{inter}}}$  is the intermediate activation vector from the input space  $\mathbb{X}_d \subseteq \mathbb{R}^{d_{\text{inter}}}$  and  $\mathbf{U} \in \mathbb{R}^{d_{\text{inter}} \times d_{\text{inter}}}$  is a diagonal matrix determining which  $r$  columns of  $\mathbf{W}_d$  to keep.

**Lemma 4** (Equivalent form of Problem 3). *The objective in Problem 3 is equivalent to the following:*

$$\operatorname{argmin}_{\mathbf{U}=\operatorname{diag}(u_1, u_2, \dots, u_{d_{\text{inter}}})} \|\mathbf{R}_{\mathbb{X}_d \mathbb{X}_d}^{\frac{1}{2}} \mathbf{U} \mathbf{W}_d - \mathbf{R}_{\mathbb{X}_d \mathbb{X}_d}^{\frac{1}{2}} \mathbf{W}_d\|_F^2 \quad \text{s.t.} \quad \operatorname{rank}(\mathbf{U}) = r, \quad (19)$$

where  $\mathbf{R}_{\mathbb{X}_d \mathbb{X}_d} := \mathbb{E}_{\mathbf{x}_d \sim \mathbb{X}_d} \{ \mathbf{x}_d^T \mathbf{x}_d \}$  is the autocorrelation matrix of the input space  $\mathbb{X}_d$ .

The derivation of Lemma 4 is in Appendix B.3.1. This CUR approximation is a well-studied NP-hard problem, and various CUR methods have been proposed [Boutsidis and Woodruff, 2014, Drineas et al., 2006]. We thus pick a simple but effective solution from Drineas et al. [2006] and name this approach A<sup>3</sup>-MLP.

Following Drineas et al. [2006], we build  $\mathbf{U}$  by sorting the F-norm of the outer product between the columns of  $\mathbf{R}_{\mathbb{X}_d \mathbb{X}_d}^{\frac{1}{2}}$  and the rows of  $\mathbf{W}_d$ :

$$\lambda_i = \|\mathbf{r}_i^T \mathbf{w}_i\|_F^2 = \|\mathbf{r}_i\|_2^2 \cdot \|\mathbf{w}_i\|_2^2, \quad (20)$$

where  $\mathbf{r}_i$  is the  $i$ -th column of  $\mathbf{R}_{\mathbb{X}_d \mathbb{X}_d}^{\frac{1}{2}}$  and  $\mathbf{w}_i$  is the  $i$ -th row of  $\mathbf{W}_d$ . Then  $\mathbf{U}$  is built by selecting the indexes that gives the top- $r$   $\lambda_i$ :

$$\mathbf{U} = \operatorname{diag}(u_1, u_2, \dots, u_{d_{\text{inter}}}) \quad \text{where} \quad u_i = \frac{1}{r \lambda_i} \text{ if } i \in \text{top-}r(\lambda_i) \text{ else } 0. \quad (21)$$

In practice, we calibrate  $\mathbb{R}_{\mathbb{X}_d \mathbb{X}_d}$  on a calibration set and compute  $\lambda_i$  for all  $i = 1, \dots, d_{\text{inter}}$ . Then we select the  $r$  rows of  $\mathbf{W}_d$  that has non-zero  $\lambda_i$  to form  $\tilde{\mathbf{W}}_d \in \mathbb{R}^{r \times d_m}$ . Accordingly,  $\tilde{\mathbf{W}}_u, \tilde{\mathbf{W}}_g \in \mathbb{R}^{d_m \times r}$  are formed by selecting the corresponding columns of  $\mathbf{W}_u$  and  $\mathbf{W}_g$  respectively.

Note that most related works, *e.g.*, the ones introduced in Section 2, target general linear layers and replace a weight matrix with two low-rank matrices  $\mathbf{X} \mathbf{W} \approx (\mathbf{X} \mathbf{A}_r) \mathbf{B}_r$ , which introduces one more GEMM operation per linear layer at inference time. In contrast, *all of our three solutions only reduce the hidden dimensions of the components ( $h_q$ ,  $d_{\text{vo}}$ , and  $d_{\text{inter}}$ ), resulting in the same number of GEMM operations with smaller problem sizes. This naturally enables reduced model sizes, saved the FLOPs of both linear layers and attention, compressed KV cache, without introducing any runtime overhead.*

### 3.4 Adapting A<sup>3</sup> for GQA and RoPE

Our A<sup>3</sup>-QK and A<sup>3</sup>-OV described above is for standard MHA. In this subsection, we extend A<sup>3</sup> for GQA and RoPE, enabling A<sup>3</sup> to be applied to a wider range of models.

**Joint SVD for GQA (A<sup>3</sup>-QK and A<sup>3</sup>-OV for GQA-NoPE)** In GQA, a key head is shared with multiples query heads in the same QK group. This grouping prevents us from applying Theorem 2 to each QK head independently. Inspired by [Ji et al., 2025], we first concatenate the scaled error matrices in Equation (12) within the same QK group and apply joint SVD:

$$\text{SVD} \left( \begin{bmatrix} \mathbf{R}_{\mathbb{X}_q \mathbb{X}_q}^{\frac{1}{2}} \mathbf{W}_{\text{qk},1} \mathbf{R}_{\mathbb{X}_{\text{kv}} \mathbb{X}_{\text{kv}}}^{\frac{1}{2}} \\ \vdots \\ \mathbf{R}_{\mathbb{X}_q \mathbb{X}_q}^{\frac{1}{2}} \mathbf{W}_{\text{qk},g} \mathbf{R}_{\mathbb{X}_{\text{kv}} \mathbb{X}_{\text{kv}}}^{\frac{1}{2}} \end{bmatrix} \right) = \mathbf{U} \mathbf{\Sigma} \mathbf{V}^T, \quad (22)$$

where  $g := \lfloor h_q / h_{\text{kv}} \rfloor$  is the number of query heads in this group. Then for this group, we assign

$$\tilde{\mathbf{W}}_{\text{qk},i} := \mathbf{R}_{\mathbb{X}_q \mathbb{X}_q}^{\frac{1}{2}} U_{id_m:(i+1)d_m, :r}^{-1}, \quad \tilde{\mathbf{W}}_{\text{k}, \text{shared}} := \mathbf{\Sigma}_{:,r, :r} V_{:,r, :d_m}^T \left( \mathbf{R}_{\mathbb{X}_{\text{kv}} \mathbb{X}_{\text{kv}}}^{\frac{1}{2}} \right)^{-1}, \quad (23)$$

to build the  $i$ -th head's approximated query weights  $\tilde{\mathbf{W}}_{\text{qk},i}$  and the shared head key weights  $\tilde{\mathbf{W}}_{\text{k}, \text{shared}}$ . The subscript with colons, *e.g.*,  $\mathbf{\Sigma}_{:,r, :r}$ , denotes array slicing. Similarly, we can apply joint SVD to the OV component by concatenating the scaled error matrices along the column dimension. A detailed description can be found in Appendix B.4.

**CUR Approximation for MHA with RoPE (A<sup>3</sup>-QK for RoPE)** Recent works have shown that not all RoPE frequencies are helpful for the model performance [Barbero et al., 2024, Ji et al., 2025]. These findings motivate our adaptation of A<sup>3</sup>-QK for attention with RoPE. RoPE inserts a position-dependent operation before the dot product between queries and keys:

$$\text{RoPE}(\mathbf{q}_{q,i}, m, \mathbf{k}_{k,i}, n) = \mathbf{q}_{q,i} \Phi_m \Phi_n^T \mathbf{k}_{k,i}^T, \quad (24)$$

where  $m$  and  $n$  are the position indexes of  $\mathbf{q}_{q,i}$  and  $\mathbf{k}_{k,i}$ ,  $\Phi_m, \Phi_n \in \mathbb{R}^{d_{qk} \times d_{qk}}$  are matrices rotating adjacent pairs of query elements and key elements. To deal with these pairwise rotations, we use CUR approximation to solve the problem in Lemma 1. Similar to A<sup>3</sup>-MLP, we seek for a rank- $r$  CUR approximation of  $(\mathbf{R}_{\mathbb{X}_q \mathbb{X}_q}^{\frac{1}{2}} \mathbf{W}_{q,i})(\mathbf{W}_{k,i}^T \mathbf{R}_{\mathbb{X}_{kv} \mathbb{X}_{kv}}^{\frac{1}{2}})$  that extracts the most important head dimensions as well as RoPE frequencies. Assign  $\mathbf{L} := \mathbf{R}_{\mathbb{X}_q \mathbb{X}_q}^{\frac{1}{2}} \mathbf{W}_{q,i}$  and  $\mathbf{R} = \mathbf{W}_{k,i}^T \mathbf{R}_{\mathbb{X}_{kv} \mathbb{X}_{kv}}^{\frac{1}{2}}$ , the objective is

$$\text{argmin}_{\mathbf{U}=\text{diag}(u_1, u_2, \dots, u_{d_{qk}})} \|\mathbf{LUR} - \mathbf{LR}\|_F^2 \quad \text{s.t.} \quad \text{rank}(\mathbf{U}) = r, \quad (25)$$

Instead of sorting by the product of  $l_2$ -norm,  $\lambda_i = \|\mathbf{L}_{:,i}\|_2 \cdot \|\mathbf{R}_{i,:}\|_2$ , for  $i = 0, 1, \dots, d_{qk} - 1$ , we sort by the sum of  $\lambda_i$  of adjacent pairs (Check Appendix B.5). This will drop pairs of less important columns in  $\mathbf{L}$  and rows in  $\mathbf{R}$ , as well as the corresponding pairs of RoPE frequencies. Our adaptation for RoPE can be combined with the joint SVD for GQA, allowing A<sup>3</sup> to be applied to various models. The evaluation in Section 4 includes standard MHA, MHA with RoPE, and GQA with RoPE.

## 4 Experiments

**Baselines** We compare A<sup>3</sup> against a range of baselines, including vanilla low-rank approximation using SVD and weight-magnitude-based column/row pruning, as well as SoTA approaches, including FWSVD [Hsu et al., 2022], ASVD [Yuan et al., 2023], SVD-LLM [Wang et al., 2024], SVD-LLM v2 [Wang et al., 2024], Palu [Chang et al., 2024], Wanda [Sun et al., 2023], and CLOVER [Meng and Zhang]. However, only several baselines support approximating all the three components (QK, OV, MLP), including SVD, FWSVD, ASVD, SVD-LLM, and SVD-LLM-v2. We conduct a comprehensive comparison against these methods. For other baselines, we align the components to approximate and present results in the ablation study.

**Models and benchmarks** Our evaluation covers vanilla Transformer and its variants, including MHA without RoPE, denoted as MHA-NoPE, (MPT [Team et al., 2023]), MHA-RoPE (LLaMA 1&2 [Touvron et al., 2023a,b]), and GQA-RoPE (LLaMA 3.1 [Grattafiori et al., 2024]). We evaluate on pretraining tasks (WikiText-2 [Merity et al., 2016], C4 [Raffel et al., 2020], and SlimPajama [Shen et al., 2023]) using SVD-LLM’s perplexity evaluation code snippet, and downstream tasks (ARC-Challenge, BoolQ, Winogrande, GSM8K (strict match), and MMLU) using `lm-eval-harness` [Gao et al., 2024]. All experiments are post-training low-rank approximation *without fine-tuning*. We use 128 random 2048-token sequences from SlimPajama for all evaluations, except in Figure 2, where we calibrate on WikiText2 to match SVD-LLM’s setup (see Appendix C for details).

### 4.1 Main Results

This section presents the main evaluation results where we compare A<sup>3</sup> against all the baselines that can be applied to all of the three main components (QK, OV, MLP) in Transformer. We first simply evaluate on LLaMA-7B and eliminate less promising baselines, then conduct a comprehensive evaluation on more models and tasks. Lastly, we present profiling results to highlight A<sup>3</sup>’s improvement on hardware efficiency.

**Preliminary experiments** We first apply plain SVD, FWSVD, SVD-LLM, and A<sup>3</sup> on LLaMA-7B with 20%, 40%, and 60% compression ratios and compare the perplexity (PPL ↓) results on WikiText-2 to find the most promising baselines. As shown in Figure 2, SVD-LLM and A<sup>3</sup> achieve perplexities smaller than others by two to three orders of magnitude. We thus conduct further experiments on SVD-LLM and A<sup>3</sup>.

**Pretraining tasks and downstream tasks** In Table 1, we include more models to compare  $A^3$  against SVD-LLM on WikiText-2, C4, and SlimPajama, covering MHA-RoPE and GQA-RoPE architectures.  $A^3$  outperforms SVD-LLM by a large margin most of the time. Remarkably,  $A^3$  achieves a perplexity of 4.69 on WikiText-2 with LLaMA 3.1-70B, which is 3.18 lower than SVD-LLM’s 7.87 (a perplexity reduction of 58.6%) at 10% compression ratio. We present the downstream task results in Table 2, where  $A^3$  consistently outperforms SVD-LLM in terms of average accuracy ( $\uparrow$ ) across all five tasks. We observe that the advantage of  $A^3$  is more pronounced when the compression ratio is small (10%). We attribute this to the adaptation of  $A^3$  for RoPE and GQA, which we will discuss in Section 4.2.

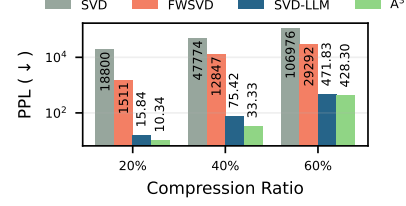


Figure 2: LLaMA-7b PPL on C4, compared to SVD, FWSVD and SVD-LLM.

Table 1: A comparison of perplexity ( $\downarrow$ ) on WikiText2, C4, and SlimPajama.

Model	Method	10%			20%		
		WikiText-2	C4	SlimPajama	WikiText-2	C4	SlimPajama
LLaMA-2-7B (MHA-RoPE)	SVD-LLM	8.78 (+3.30)	11.73 (+4.14)	9.49 (+3.35)	11.58 (+6.1)	14.91 (+7.32)	11.93 (+5.79)
	$A^3$	<b>5.96 (+0.48)</b>	<b>8.34 (+0.74)</b>	<b>6.68 (+0.54)</b>	<b>7.22 (+1.73)</b>	<b>9.91 (+2.31)</b>	<b>7.91 (+1.77)</b>
LLaMA-2-13B (MHA-RoPE)	SVD-LLM	7.09 (+2.19)	9.98 (+2.92)	7.95 (+2.26)	9.03 (+4.13)	12.35 (+5.29)	9.75 (+4.06)
	$A^3$	<b>5.32 (+0.42)</b>	<b>7.65 (+0.59)</b>	<b>7.65 (+1.97)</b>	<b>6.24 (+1.34)</b>	<b>8.99 (+1.92)</b>	<b>7.15 (+1.47)</b>
LLaMA-3.1-8B (GQA-RoPE)	SVD-LLM	19.12 (+12.86)	19.37 (+9.33)	15.14 (+7.57)	42.28 (+36.02)	33.6 (+23.56)	27.44 (+19.86)
	$A^3$	<b>7.93 (+1.67)</b>	<b>12.56 (+2.52)</b>	<b>9.52 (+1.94)</b>	<b>11.36 (+5.1)</b>	<b>17.87 (+10.29)</b>	<b>13.58 (+3.54)</b>
LLaMA-3.1-70B (GQA-RoPE)	SVD-LLM	7.87 (+5.07)	11.3 (+3.76)	8.43 (+2.94)	9.75 (+6.95)	<b>13.77 (+6.23)</b>	10.44 (+4.95)
	$A^3$	<b>4.69 (+1.90)</b>	<b>8.83 (+1.31)</b>	<b>6.59 (+1.10)</b>	<b>8.32 (+5.52)</b>	13.94 (+6.40)	<b>10.02 (+4.53)</b>

**Higher inference throughput** The low-rank approximation methods that target general linear layers only save the FLOPs of GEMM in linear layers, but induce runtime overhead like extra GEMM kernel launches and read/write for small matrices. In contrast,  $A^3$  saves the GEMM FLOPs in both linear layers and attention, without inducing these overheads. We profile prefilling throughput measured in TPS (tokens/sec) of LLaMA-2-13B on an A100 40GB, and visualize the speedup in Figure 3. SVD-LLM only has speedup for aggressive compression, while  $A^3$  always achieves a speedup, higher than SVD-LLM.

Table 2: A comparison of downstream task accuracy ( $\uparrow$ ).

Model	CRatio	Method	ARC-c	BoolQ	Winogrande	GSM8k	MMLU	Avg.
LLaMA-2-7b (MHA-RoPE)	-	Original	0.4829	0.7777	0.7498	0.1387	0.4582	0.5158
	10%	SVD-LLM	0.3882	0.6749	0.6803	0.0129	0.3477	0.4166
		A <sup>3</sup>	<b>0.4761</b>	<b>0.7330</b>	<b>0.7435</b>	<b>0.1130</b>	<b>0.4398</b>	<b>0.4960</b>
	20%	SVD-LLM	0.3139	0.6602	0.6464	0.0045	0.3119	0.3837
A <sup>3</sup>		<b>0.4369</b>	<b>0.7174</b>	<b>0.7072</b>	<b>0.0751</b>	<b>0.3979</b>	<b>0.4621</b>	
LLaMA-2-13b (MHA-RoPE)	-	Original	0.5538	0.8086	0.7711	0.2343	0.5513	0.5774
	10%	SVD-LLM	0.4206	<b>0.8061</b>	0.7308	0.0902	0.4772	0.5000
		A <sup>3</sup>	<b>0.5213</b>	0.7865	<b>0.7743</b>	<b>0.1971</b>	<b>0.5324</b>	<b>0.5560</b>
	20%	SVD-LLM	0.3472	<b>0.7877</b>	0.6898	0.0379	0.4318	0.4546
A <sup>3</sup>		<b>0.4727</b>	0.7654	<b>0.7364</b>	<b>0.1645</b>	<b>0.4804</b>	<b>0.5180</b>	
LLaMA-3.1-8B (GQA-RoPE)	-	Original	0.5401	0.8190	0.7822	0.4920	0.6535	0.6484
	10%	SVD-LLM	0.3575	0.7458	<b>0.7111</b>	0.0447	0.4708	0.4603
		A <sup>3</sup>	<b>0.4565</b>	<b>0.7884</b>	0.7072	<b>0.2388</b>	<b>0.5922</b>	<b>0.5500</b>
	20%	SVD-LLM	0.2534	<b>0.6948</b>	<b>0.6440</b>	0.0113	0.3604	0.3880
A <sup>3</sup>		<b>0.3345</b>	0.6823	0.6417	<b>0.0705</b>	<b>0.4649</b>	<b>0.4336</b>	
LLaMA-3.1-70B (GQA-RoPE)	-	Original	0.6536	0.8538	0.8445	0.8036	0.7864	0.7768
	10%	SVD-LLM	0.5742	0.8401	0.8051	0.5087	0.7181	0.6797
		A <sup>3</sup>	<b>0.6323</b>	<b>0.8532</b>	<b>0.8335</b>	<b>0.7453</b>	<b>0.7470</b>	<b>0.7508</b>
	20%	SVD-LLM	<b>0.4957</b>	<b>0.8226</b>	<b>0.7727</b>	0.3040	<b>0.6620</b>	0.6025
A <sup>3</sup>		0.4667	0.8144	0.6875	<b>0.4951</b>	0.6145	<b>0.6071</b>	



## 4.2 Ablation Study and Improvement over other Baselines

We conduct ablation studies to evaluate  $A^3$ 's impact on individual components (QK, OV, MLP). We also include baselines that can be applied to the target components to show  $A^3$ 's advantage.

**Attention without RoPE** Theorem 2 ( $A^3$ -QK) and Theorem 3 ( $A^3$ -OV) provide optimal solutions for MHA-NoPE's QK and OV components without the need of adaptation. We evaluate the increased perplexity ( $\Delta PPL \downarrow$ ) of  $A^3$ -QK and  $A^3$ -OV on MPT-7B (MHA-NoPE) in Figure 4a, comparing against CLOVER [Meng and Zhang] and Palu [Chang et al., 2024], with compression ratio=20%. CLOVER is equivalent to  $A^3$ -QK but assumes  $R_{\mathbb{X}_{q,q}}$  and  $R_{\mathbb{X}_{kv,kv}}$  are identity matrices (no activation information). The bars are grouped by the component being approximated (QK, OV).

We add two bars representing simplified version  $A^3$ -QK in the QK group,  $A^3$ -Q-only and  $A^3$ -K-only.  $A^3$ -Q-only (K-only) replaces the autocorrelation matrix of key (query) in Equation (12) with an identity matrix. We also add a simplified version  $A^3$ -OV in the OV group,  $A^3$ -Xkv, which replaces the autocorrelation matrix of  $p_i$  in Equation (17) with the autocorrelation matrix of  $x_{kv}$ . The auto-correlation matrices of these simplified versions of  $A^3$  are cheaper to calibrate. We observe that  $A^3$ -QK-SVD and  $A^3$ -OV-SVD and their simplified versions outperform CLOVER and Palu by a clear margin.

**Attention with RoPE** In Section 3.4 we propose using CUR approximation to solve Problem 1 for attention with RoPE, which follows a similar approach as  $A^3$ -MLP in Section 3.3. Here we compare against structured pruning baselines that can be adapted for this problem, including  $\text{abs}(w)$  and Wanda [Sun et al., 2023].  $\text{abs}(w)$  represents the classic pruning method that drops weights with smaller magnitudes, while Wanda sorts by the product between the weight magnitude and the average  $l_2$ -norm of the corresponding activation row<sup>1</sup>. Figure 4b illustrates  $\Delta PPL$  of LLaMA-2-7B on WikiText2, indicating the advantage of  $A^3$  over  $\text{abs}(w)$  and Wanda.

## 5 Discussion

In Appendix D, we showcase various applications of  $A^3$ , highlighting its compatibility with quantization and extensibility to mixed-rank allocation for additional performance gains. We find  $A^3$  is orthogonal to weight-only quantization methods like HQQ [Badri and Shaji, 2023], and a simple mixed-rank  $A^3$  outperforms ASVD and SVD-LLM v2. We also discuss the limitations of  $A^3$  in Appendix D, mainly caused by the sub-optimality of CUR decomposition, a compromise to RoPE. Finally, we explore the impact of calibration set selection on overall method performance, showing that a mixture of calibration datasets boosts accuracies on downstream tasks like Winogrande.

## 6 Conclusion

We propose  $A^3$ , an analytical framework that decomposes the transformer into its core components, **QK**, **OV**, **MLP**, and compresses them by minimizing their respective errors. This method reduces model size, KV cache, and FLOPs without runtime overhead, while achieving state-of-the-art performance.

<sup>1</sup>In the case of Equation (25),  $\text{abs}(w)$  drops columns (rows) by the column (row) sum of magnitudes of  $W_{q,i}$  ( $W_{k,i}^T$ ), while Wanda assumes non-diagonal elements in  $R_{\mathbb{X}_{q,q}}$  and  $R_{\mathbb{X}_{kv,kv}}$  are all zeros.

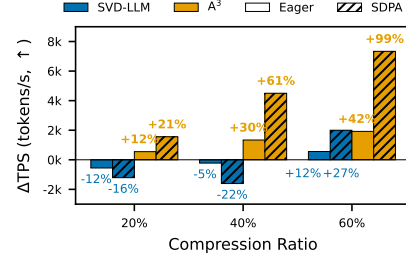
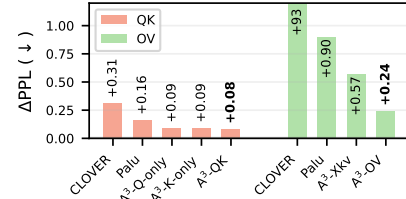
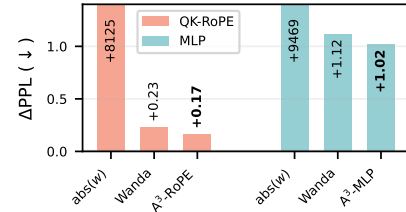


Figure 3: Performance comparisons in Tokens per Second (TPS) of  $A^3$  and SVD-LLM (LLaMA-2-13b, A100 40GB, batch size=2, sequence length=2048, attention backend=Eager/SDPA).



(a) QK and OV (MHA-NoPE).



(b) QK-RoPE and MLP (MHA-RoPE).

Figure 4: Ablation study of  $A^3$  components. (a) QK and OV on MPT-7B. (b) QK-RoPE and MLP on LLaMA-2-7B.

## References

- Joshua Ainslie, James Lee-Thorp, Michiel De Jong, Yury Zemlyanskiy, Federico Lebrón, and Sumit Sanghai. Gqa: Training generalized multi-query transformer models from multi-head checkpoints. *arXiv preprint arXiv:2305.13245*, 2023.
- Hicham Badri and Appu Shaji. Half-quadratic quantization of large machine learning models. *Dan Hendrycks, Collin Burns, Steven Basart, Andy Zou, Mantas Mazeika, Dawn Song, and Jacob*, 2023.
- Federico Barbero, Alex Vitvitskyi, Christos Perivolaropoulos, Razvan Pascanu, and Petar Veličković. Round and round we go! what makes rotary positional encodings useful? *arXiv preprint arXiv:2410.06205*, 2024.
- Christos Boutsidis and David P Woodruff. Optimal cur matrix decompositions. In *Proceedings of the forty-sixth annual ACM symposium on Theory of computing*, pages 353–362, 2014.
- Tom Brown, Benjamin Mann, Nick Ryder, Melanie Subbiah, Jared D Kaplan, Prafulla Dhariwal, Arvind Neelakantan, Pranav Shyam, Girish Sastry, Amanda Askell, et al. Language models are few-shot learners. *Advances in neural information processing systems*, 33:1877–1901, 2020.
- Chi-Chih Chang, Wei-Cheng Lin, Chien-Yu Lin, Chong-Yan Chen, Yu-Fang Hu, Pei-Shuo Wang, Ning-Chi Huang, Luis Ceze, Mohamed S Abdelfattah, and Kai-Chiang Wu. Palu: Compressing kv-cache with low-rank projection. *arXiv preprint arXiv:2407.21118*, 2024.
- Mark Chen, Jerry Tworek, Heewoo Jun, Qiming Yuan, Henrique Ponde De Oliveira Pinto, Jared Kaplan, Harri Edwards, Yuri Burda, Nicholas Joseph, Greg Brockman, et al. Evaluating large language models trained on code. *arXiv preprint arXiv:2107.03374*, 2021a.
- Patrick Chen, Hsiang-Fu Yu, Inderjit Dhillon, and Cho-Jui Hsieh. Drone: Data-aware low-rank compression for large nlp models. *Advances in neural information processing systems*, 34:29321–29334, 2021b.
- Petros Drineas, Ravi Kannan, and Michael W Mahoney. Fast monte carlo algorithms for matrices i: Approximating matrix multiplication. *SIAM Journal on Computing*, 36(1):132–157, 2006.
- Carl Eckart and Gale Young. The approximation of one matrix by another of lower rank. *Psychometrika*, 1(3):211–218, 1936a.
- Carl Eckart and Gale Young. The approximation of one matrix by another of lower rank. *Psychometrika*, 1(3):211–218, 1936b.
- Nelson Elhage, Neel Nanda, Catherine Olsson, Tom Henighan, Nicholas Joseph, Ben Mann, Amanda Askell, Yuntao Bai, Anna Chen, Tom Conerly, et al. A mathematical framework for transformer circuits. *Transformer Circuits Thread*, 1(1):12, 2021.
- Leo Gao, Jonathan Tow, Baber Abbasi, Stella Biderman, Sid Black, Anthony DiPofi, Charles Foster, Laurence Golding, Jeffrey Hsu, Alain Le Noac’h, Haonan Li, Kyle McDonell, Niklas Muennighoff, Chris Ociepa, Jason Phang, Laria Reynolds, Hailey Schoelkopf, Aviya Skowron, Lintang Sutawika, Eric Tang, Anish Thite, Ben Wang, Kevin Wang, and Andy Zou. The language model evaluation harness, 07 2024. URL <https://zenodo.org/records/12608602>.
- Aaron Grattafiori, Abhimanyu Dubey, Abhinav Jauhri, Abhinav Pandey, Abhishek Kadian, Ahmad Al-Dahle, Aiesha Letman, Akhil Mathur, Alan Schelten, Alex Vaughan, et al. The llama 3 herd of models. *arXiv preprint arXiv:2407.21783*, 2024.
- Yen-Chang Hsu, Ting Hua, Sungen Chang, Qian Lou, Yilin Shen, and Hongxia Jin. Language model compression with weighted low-rank factorization. *arXiv preprint arXiv:2207.00112*, 2022.
- Tao Ji, Bin Guo, Yuanbin Wu, Qipeng Guo, Lixing Shen, Zhan Chen, Xipeng Qiu, Qi Zhang, and Tao Gui. Towards economical inference: Enabling deepseek’s multi-head latent attention in any transformer-based llms. *arXiv preprint arXiv:2502.14837*, 2025.

- Aixin Liu, Bei Feng, Bing Xue, Bingxuan Wang, Bochao Wu, Chengda Lu, Chenggang Zhao, Chengqi Deng, Chenyu Zhang, Chong Ruan, et al. Deepseek-v3 technical report. *arXiv preprint arXiv:2412.19437*, 2024.
- Michael W Mahoney and Petros Drineas. Cur matrix decompositions for improved data analysis. *Proceedings of the National Academy of Sciences*, 106(3):697–702, 2009.
- Fanxu Meng and Muhan Zhang. Clover: Cross-layer orthogonal vectors pruning and fine-tuning. In *The Fourth Blogpost Track at ICLR 2025*.
- Stephen Merity, Caiming Xiong, James Bradbury, and Richard Socher. Pointer sentinel mixture models. *arXiv preprint arXiv:1609.07843*, 2016.
- Colin Raffel, Noam Shazeer, Adam Roberts, Katherine Lee, Sharan Narang, Michael Matena, Yanqi Zhou, Wei Li, and Peter J Liu. Exploring the limits of transfer learning with a unified text-to-text transformer. *Journal of machine learning research*, 21(140):1–67, 2020.
- Rajarshi Saha, Naomi Sagan, Varun Srivastava, Andrea Goldsmith, and Mert Pilanci. Compressing large language models using low rank and low precision decomposition. *Advances in Neural Information Processing Systems*, 37:88981–89018, 2024.
- Noam Shazeer. Fast transformer decoding: One write-head is all you need. *arXiv preprint arXiv:1911.02150*, 2019.
- Noam Shazeer. Glu variants improve transformer. *arXiv preprint arXiv:2002.05202*, 2020.
- Zhiqiang Shen, Tianhua Tao, Liqun Ma, Willie Neiswanger, Zhengzhong Liu, Hongyi Wang, Bowen Tan, Joel Hestness, Natalia Vassilieva, Daria Soboleva, et al. Slimpajama-dc: Understanding data combinations for llm training. *arXiv preprint arXiv:2309.10818*, 2023.
- Jianlin Su, Murtadha Ahmed, Yu Lu, Shengfeng Pan, Wen Bo, and Yunfeng Liu. Roformer: Enhanced transformer with rotary position embedding. *Neurocomputing*, 568:127063, 2024.
- Mingjie Sun, Zhuang Liu, Anna Bair, and J Zico Kolter. A simple and effective pruning approach for large language models. *arXiv preprint arXiv:2306.11695*, 2023.
- MosaicML NLP Team et al. Introducing mpt-7b: A new standard for open-source, commercially usable llms. *DataBricks (May, 2023)* [www.mosaicml.com/blog/mpt-7b](http://www.mosaicml.com/blog/mpt-7b), 2023.
- Hugo Touvron, Thibaut Lavril, Gautier Izacard, Xavier Martinet, Marie-Anne Lachaux, Timothée Lacroix, Baptiste Rozière, Naman Goyal, Eric Hambro, Faisal Azhar, et al. Llama: Open and efficient foundation language models. *arXiv preprint arXiv:2302.13971*, 2023a.
- Hugo Touvron, Louis Martin, Kevin Stone, Peter Albert, Amjad Almahairi, Yasmine Babaei, Nikolay Bashlykov, Soumya Batra, Prajjwal Bhargava, Shruti Bhosale, et al. Llama 2: Open foundation and fine-tuned chat models. *arXiv preprint arXiv:2307.09288*, 2023b.
- Ashish Vaswani, Noam Shazeer, Niki Parmar, Jakob Uszkoreit, Llion Jones, Aidan N Gomez, Łukasz Kaiser, and Illia Polosukhin. Attention is all you need. *Advances in neural information processing systems*, 30, 2017.
- Xin Wang, Yu Zheng, Zhongwei Wan, and Mi Zhang. Svd-llm: Truncation-aware singular value decomposition for large language model compression. *arXiv preprint arXiv:2403.07378*, 2024.
- Xin Wang, Samiul Alam, Zhongwei Wan, Hui Shen, and Mi Zhang. Svd-llm v2: Optimizing singular value truncation for large language model compression. *arXiv preprint arXiv:2503.12340*, 2025.
- Jason Wei, Xuezhi Wang, Dale Schuurmans, Maarten Bosma, Fei Xia, Ed Chi, Quoc V Le, Denny Zhou, et al. Chain-of-thought prompting elicits reasoning in large language models. *Advances in neural information processing systems*, 35:24824–24837, 2022.
- Zhihang Yuan, Yuzhang Shang, Yue Song, Qiang Wu, Yan Yan, and Guangyu Sun. Asvd: Activation-aware singular value decomposition for compressing large language models. *arXiv preprint arXiv:2312.05821*, 2023.

Cheng Zhang, Jianyi Cheng, George A Constantinides, and Yiren Zhao. Lqer: Low-rank quantization error reconstruction for llms. *arXiv preprint arXiv:2402.02446*, 2024a.

Cheng Zhang, Jeffrey TH Wong, Can Xiao, George A Constantinides, and Yiren Zhao. Qera: an analytical framework for quantization error reconstruction. *arXiv preprint arXiv:2410.06040*, 2024b.

## A Notations

Table 3 includes the notations of matrices and vectors and Table 4 summarizes the notations of dimensions in this paper.

Table 3: Notation of matrices and vectors in this paper.

Notation	Description
$\mathbf{R}_{\mathbb{X}\mathbb{X}}$	The autocorrelation matrices of the input spaces $\mathbb{X}$ , computed as $\mathbb{E}_{\mathbf{x} \sim \mathbb{X}} \{ \mathbf{x}^T \mathbf{x} \}$
$\mathbf{R}_{\mathbb{X}\mathbb{X}}^{\frac{1}{2}}$	The corresponding unique symmetric matrix square roots of $\mathbf{R}_{\mathbb{X}\mathbb{X}}$
$\mathbf{q}_{q,i}$	An input vector to query projection of $i$ -th head
$\mathbf{k}_{k,i}$	An input vector to key/value projection of $i$ -th head
$\mathbf{W}_{q,i}$	Weight of query projection of $i$ -th head
$\mathbf{W}_{k,i}$	Weight of key projection of $i$ -th head
$\mathbf{W}_{\text{qk},i}$	Fused weight of query/key projection of $i$ -th head
$\widetilde{\mathbf{W}}_{\text{qk},i}$	Low-rank approximation of $\mathbf{W}_{\text{qk},i}$
$\widetilde{\mathbf{W}}_{q,i}$	Approximated $\mathbf{W}_{q,i}$ , left low-rank matrix of $\widetilde{\mathbf{W}}_{\text{qk},i}$
$\widetilde{\mathbf{W}}_{k,i}$	Approximated $\mathbf{W}_{k,i}$ , right low-rank matrix of $\widetilde{\mathbf{W}}_{\text{qk},i}$
$\mathbf{Q}_i$	Query of $i$ -th head
$\mathbf{K}_i$	Key of $i$ -th head
$a_i$	A single attention score of $i$ -th head
$\mathbf{A}_i$	Pre-softmax attention score of $i$ -th head
$\mathbf{A}'_i$	Post-softmax attention score of $i$ -th head
$\mathbf{W}_{v,i}$	Weight of value projection of $i$ -th head
$\mathbf{W}_{o,i}$	Weight of output projection of $i$ -th head
$\mathbf{W}_{\text{vo},i}$	Fused weight of value/output projection of $i$ -th head
$\widetilde{\mathbf{W}}_{\text{vo},i}$	Low-rank approximation of $\mathbf{W}_{\text{vo},i}$
$\mathbf{o}$	A row of attention output
$\mathbf{o}_i$	A row of attention output $i$ -th head
$\widetilde{\mathbf{o}}$	Low-rank approximation of $\mathbf{o}$
$\mathbf{O}$	Attention output matrix
$\mathbf{x}_d$	Input vectors of down projection layer in MLP
$\widetilde{\mathbf{x}}_d$	Input vectors of down projection layer in MLP after low-rank approximation
$\mathbf{y}_{\text{mlp}}$	Output vectors of down projection layer in MLP after low-rank approximation
$\mathbf{X}_{\text{mlp}}$	Input of MLP in transformer
$\mathbf{X}_d$	Input of down projection layer in MLP
$\mathbf{Y}_d$	Output of gate projection layer in MLP
$\mathbf{Y}_u$	Output of up projection layer in MLP
$\mathbf{Y}_{\text{mlp}}$	Output of down projection layer in MLP
$\mathbf{W}_u$	Weight of up projection layer in MLP
$\mathbf{W}_d$	Weight of down projection layer in MLP
$\mathbf{W}_g$	Weight of gate projection layer in MLP
$\widetilde{\mathbf{W}}_d$	Weight of up projection layer in low-rank approximated MLP
$\widetilde{\mathbf{W}}_d$	Weight of down projection layer in low-rank approximated MLP
$\widetilde{\mathbf{W}}_d$	Weight of gate projection layer in low-rank approximated MLP
$\mathbf{r}_i$	The $i$ -th columns of $\mathbf{R}_{\mathbb{X}_d \mathbb{X}_d}^{\frac{1}{2}}$
$\mathbf{w}_i$	The $i$ -th rows of $\mathbf{W}_d$

Table 4: Notation of dimensions in this paper.

Notation	Description
$l_q$	Query sequence length
$l_{kv}$	Key and value sequence length
$d_m$	Model hidden size
$h_q$	Number of attention (query) heads
$h_{kv}$	Number of key and value heads
$g := \lfloor h_q/h_{kv} \rfloor$	Number of query heads per key/value head in GQA
$d_{vo}$	Head dimension shared by value and head output projection
$d_{qk}$	Head dimension shared by query and key
$d_{inter}$	Intermediate size of FFN

## B Derivations for $A^3$

### B.1 $A^3$ -QK

#### B.1.1 Independent Assumption Discussion of $A^3$ -QK

We model  $\mathbf{x}_q$  and  $\mathbf{x}_{kv}$  as independent samples drawn from a shared distribution in Equation (10). In this section, we examine the extent to which this assumption holds in practice. To do so, we plot the token-token correlation matrix of the hidden states in LLaMA-3.1-8B, using input sequences of length 2048 sampled from SlimPajama (see Figure 5). The results show that in the early layers, token representations are relatively uncorrelated. However, as the self-attention mechanism allows tokens to attend to one another, the model begins to encode shared contextual information. This information accumulates across layers, introducing increasing dependencies between the representations of the query and key/value pairs. As a result, the assumption of strict independence between  $\mathbf{x}_q$  and  $\mathbf{x}_{kv}$  becomes less valid in deeper layers.

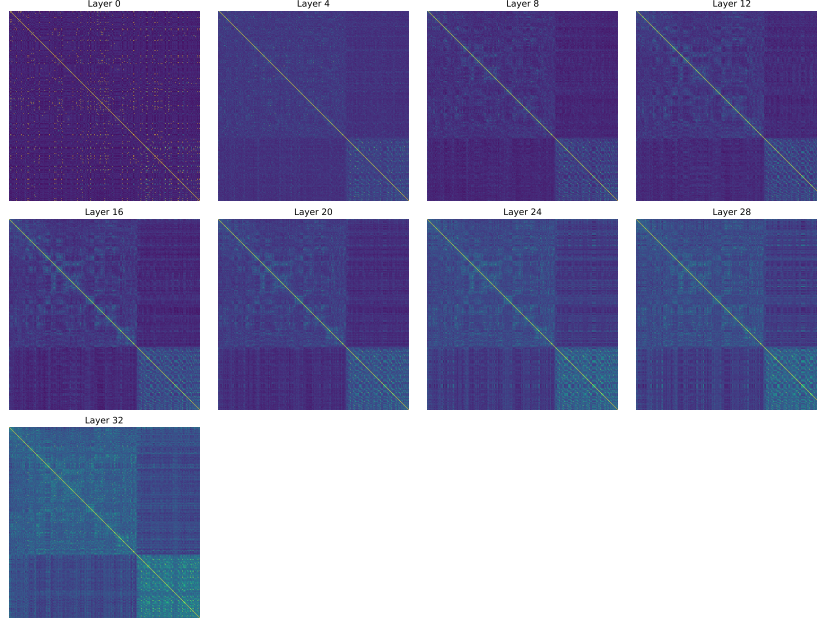


Figure 5: The  $\mathbf{x}_q$  and  $\mathbf{x}_{kv}$  covariance matrix across all decoders with a sample (2048 sequence length) from SlimPajama.

### B.1.2 Equivalent Objective

Here we provide the full derivation for Lemma 1 from Problem 1:

$$\begin{aligned} & \operatorname{argmin}_{\widetilde{\mathbf{W}}_{\mathbf{q},i}} \mathbb{E}_{\mathbf{x}_{\mathbf{q}} \sim \mathbb{X}_{\mathbf{q}}, \mathbf{x}_{\mathbf{kv}} \sim \mathbb{X}_{\mathbf{kv}}} \{(\mathbf{x}_{\mathbf{q}}(\mathbf{W}_{\mathbf{q},i} - \widetilde{\mathbf{W}}_{\mathbf{q},i})\mathbf{x}_{\mathbf{kv}}^T)^2\} \quad \text{s.t.} \quad \operatorname{rank}(\widetilde{\mathbf{W}}_{\mathbf{q},i}) = r \\ & \Rightarrow \operatorname{argmin}_{\widetilde{\mathbf{W}}_{\mathbf{q},i}} \mathbb{E}_{\mathbf{x}_{\mathbf{q}} \sim \mathbb{X}_{\mathbf{q}}, \mathbf{x}_{\mathbf{kv}} \sim \mathbb{X}_{\mathbf{kv}}} \{\|R_{\mathbb{X}_{\mathbf{q}}\mathbb{X}_{\mathbf{q}}}^{\frac{1}{2}}(\mathbf{W}_{\mathbf{q},i} - \widetilde{\mathbf{W}}_{\mathbf{q},i})R_{\mathbb{X}_{\mathbf{kv}}\mathbb{X}_{\mathbf{kv}}}^{\frac{1}{2}}\|_F^2\}. \end{aligned} \quad (26)$$

*Proof.* We begin with the right-hand side (RHS) of Equation (26). For clarity, we define some intermediate variables:

$$\mathbf{P} := [\mathbf{p}_1^T, \mathbf{p}_2^T, \dots, \mathbf{p}_{d_m}^T]^T = \mathbf{W}_{\mathbf{q},i} - \widetilde{\mathbf{W}}_{\mathbf{q},i}, \quad \mathbf{x}_{\mathbf{q}} = [x_{q,1} \quad x_{q,2} \quad \dots \quad x_{q,d_m}]^T, \quad (27)$$

Substitute Equation (27) to RHS of Equation (26):

$$\begin{aligned} & \mathbb{E}_{\mathbf{x}_{\mathbf{q}} \sim \mathbb{X}_{\mathbf{q}}, \mathbf{x}_{\mathbf{kv}} \sim \mathbb{X}_{\mathbf{kv}}} \{(\mathbf{x}_{\mathbf{q}}(\mathbf{W}_{\mathbf{q},i} - \widetilde{\mathbf{W}}_{\mathbf{q},i})\mathbf{x}_{\mathbf{kv}}^T)^2\} \\ & = \mathbb{E}_{\mathbf{x}_{\mathbf{q}} \sim \mathbb{X}_{\mathbf{q}}, \mathbf{x}_{\mathbf{kv}} \sim \mathbb{X}_{\mathbf{kv}}} \{([x_{q,1} \quad x_{q,2} \quad \dots \quad x_{q,d_m}] [\mathbf{p}_1^T, \mathbf{p}_2^T, \dots, \mathbf{p}_{d_m}^T]^T \mathbf{x}_{\mathbf{kv}}^T)^2\} \\ & = \mathbb{E}_{\mathbf{x}_{\mathbf{q}} \sim \mathbb{X}_{\mathbf{q}}, \mathbf{x}_{\mathbf{kv}} \sim \mathbb{X}_{\mathbf{kv}}} \left\{ \left( \sum_i^{d_m} x_{q,i} \mathbf{p}_i \right) \mathbf{x}_{\mathbf{kv}}^T \right\}^2 \\ & = \mathbb{E}_{\mathbf{x}_{\mathbf{q}} \sim \mathbb{X}_{\mathbf{q}}, \mathbf{x}_{\mathbf{kv}} \sim \mathbb{X}_{\mathbf{kv}}} \{e((\mathbf{x}_{\mathbf{q}}^T \mathbf{x}_{\mathbf{q}}) \odot (\mathbf{P} \mathbf{x}_{\mathbf{kv}}^T \mathbf{x}_{\mathbf{kv}} \mathbf{P}^T))e^T\} \\ & = \mathbb{E}_{\mathbf{x}_{\mathbf{q}} \sim \mathbb{X}_{\mathbf{q}}, \mathbf{x}_{\mathbf{kv}} \sim \mathbb{X}_{\mathbf{kv}}} \{\operatorname{Tr}((\mathbf{x}_{\mathbf{q}}^T \mathbf{x}_{\mathbf{q}})(\mathbf{P} \mathbf{x}_{\mathbf{kv}}^T \mathbf{x}_{\mathbf{kv}} \mathbf{P}^T))\}. \end{aligned} \quad (28)$$

Assume  $\mathbf{x}_{\mathbf{q}}$  and  $\mathbf{x}_{\mathbf{kv}}$  are independent,  $\mathbb{E}_{\mathbf{x}_{\mathbf{q}} \sim \mathbb{X}_{\mathbf{q}}, \mathbf{x}_{\mathbf{kv}} \sim \mathbb{X}_{\mathbf{kv}}} \rightarrow \mathbb{E}_{\mathbf{x}_{\mathbf{q}} \sim \mathbb{X}_{\mathbf{q}}} \mathbb{E}_{\mathbf{x}_{\mathbf{kv}} \sim \mathbb{X}_{\mathbf{kv}}}$ :

$$\begin{aligned} & \mathbb{E}_{\mathbf{x}_{\mathbf{q}} \sim \mathbb{X}_{\mathbf{q}}, \mathbf{x}_{\mathbf{kv}} \sim \mathbb{X}_{\mathbf{kv}}} \{\operatorname{Tr}((\mathbf{x}_{\mathbf{q}}^T \mathbf{x}_{\mathbf{q}})(\mathbf{P} \mathbf{x}_{\mathbf{kv}}^T \mathbf{x}_{\mathbf{kv}} \mathbf{P}^T))\} \\ & = \operatorname{Tr}(\mathbb{E}_{\mathbf{x}_{\mathbf{q}} \sim \mathbb{X}_{\mathbf{q}}} \{(\mathbf{x}_{\mathbf{q}}^T \mathbf{x}_{\mathbf{q}})\} \mathbb{E}_{\mathbf{x}_{\mathbf{kv}} \sim \mathbb{X}_{\mathbf{kv}}} \{(\mathbf{P} \mathbf{x}_{\mathbf{kv}}^T \mathbf{x}_{\mathbf{kv}} \mathbf{P}^T)\}) \\ & = \operatorname{Tr}(\mathbf{R}_{\mathbb{X}_{\mathbf{q}}\mathbb{X}_{\mathbf{q}}} \mathbf{P} \mathbf{R}_{\mathbb{X}_{\mathbf{kv}}\mathbb{X}_{\mathbf{kv}}} \mathbf{P}^T) \\ & = \operatorname{Tr}((\mathbf{R}_{\mathbb{X}_{\mathbf{q}}\mathbb{X}_{\mathbf{q}}}^{\frac{1}{2}} \mathbf{P} \mathbf{R}_{\mathbb{X}_{\mathbf{kv}}\mathbb{X}_{\mathbf{kv}}}^{\frac{1}{2}})(\mathbf{R}_{\mathbb{X}_{\mathbf{q}}\mathbb{X}_{\mathbf{q}}}^{\frac{1}{2}} \mathbf{P} \mathbf{R}_{\mathbb{X}_{\mathbf{kv}}\mathbb{X}_{\mathbf{kv}}}^{\frac{1}{2}})^T) \\ & = \|\mathbf{R}_{\mathbb{X}_{\mathbf{q}}\mathbb{X}_{\mathbf{q}}}^{\frac{1}{2}}(\mathbf{W}_{\mathbf{q},i} - \widetilde{\mathbf{W}}_{\mathbf{q},i})\mathbf{R}_{\mathbb{X}_{\mathbf{kv}}\mathbb{X}_{\mathbf{kv}}}^{\frac{1}{2}}\|_F^2. \end{aligned} \quad (29)$$

□

### B.1.3 Analytical Solution

Here we provide the proof of Theorem 2:

*Proof.* We continue with Lemma 1.

$$\begin{aligned} & \operatorname{argmin}_{\widetilde{\mathbf{W}}_{\mathbf{q},i}} \|\mathbf{R}_{\mathbb{X}_{\mathbf{q}}\mathbb{X}_{\mathbf{q}}}^{\frac{1}{2}}(\mathbf{W}_{\mathbf{q},i} - \widetilde{\mathbf{W}}_{\mathbf{q},i})\mathbf{R}_{\mathbb{X}_{\mathbf{kv}}\mathbb{X}_{\mathbf{kv}}}^{\frac{1}{2}}\|_F^2 \quad \text{s.t.} \quad \operatorname{rank}(\widetilde{\mathbf{W}}_{\mathbf{q},i}) = r \\ & \Rightarrow \operatorname{argmin}_{\widetilde{\mathbf{W}}_{\mathbf{q},i}} \|\mathbf{R}_{\mathbb{X}_{\mathbf{q}}\mathbb{X}_{\mathbf{q}}}^{\frac{1}{2}} \mathbf{W}_{\mathbf{q},i} \mathbf{R}_{\mathbb{X}_{\mathbf{kv}}\mathbb{X}_{\mathbf{kv}}}^{\frac{1}{2}} - \mathbf{R}_{\mathbb{X}_{\mathbf{q}}\mathbb{X}_{\mathbf{q}}}^{\frac{1}{2}} \widetilde{\mathbf{W}}_{\mathbf{q},i} \mathbf{R}_{\mathbb{X}_{\mathbf{kv}}\mathbb{X}_{\mathbf{kv}}}^{\frac{1}{2}}\|_F^2. \end{aligned} \quad (30)$$

Note that multiplication by the invertible matrix  $\mathbf{R}_{\mathbb{X}_{\mathbf{q}}\mathbb{X}_{\mathbf{q}}}^{\frac{1}{2}}$  and  $\mathbf{R}_{\mathbb{X}_{\mathbf{kv}}\mathbb{X}_{\mathbf{kv}}}^{\frac{1}{2}}$  does not change the rank of the matrix  $\mathbf{W}_{\mathbf{q},i}$ . According to the Eckart-Young-Mirsky theorem [Eckart and Young, 1936b], the optimal rank  $r$  approximation to  $(\mathbf{R}_{\mathbb{X}_{\mathbf{q}}\mathbb{X}_{\mathbf{q}}}^{\frac{1}{2}} \mathbf{W}_{\mathbf{q},i} \mathbf{R}_{\mathbb{X}_{\mathbf{kv}}\mathbb{X}_{\mathbf{kv}}}^{\frac{1}{2}})$  is the truncated SVD of  $(\mathbf{R}_{\mathbb{X}_{\mathbf{q}}\mathbb{X}_{\mathbf{q}}}^{\frac{1}{2}} \mathbf{W}_{\mathbf{q},i} \mathbf{R}_{\mathbb{X}_{\mathbf{kv}}\mathbb{X}_{\mathbf{kv}}}^{\frac{1}{2}})$ :

$$(\mathbf{R}_{\mathbb{X}_{\mathbf{q}}\mathbb{X}_{\mathbf{q}}}^{\frac{1}{2}} \mathbf{W}_{\mathbf{q},i} \mathbf{R}_{\mathbb{X}_{\mathbf{kv}}\mathbb{X}_{\mathbf{kv}}}^{\frac{1}{2}})_r = \mathbf{U}_{:,r} \mathbf{\Sigma}_{:r,:r} \mathbf{V}_{:r,:}^T, \quad (31)$$

where  $\mathbf{U} \mathbf{\Sigma} \mathbf{V}^T = \operatorname{SVD}(\mathbf{R}_{\mathbb{X}_{\mathbf{q}}\mathbb{X}_{\mathbf{q}}}^{\frac{1}{2}} \mathbf{W}_{\mathbf{q},i} \mathbf{R}_{\mathbb{X}_{\mathbf{kv}}\mathbb{X}_{\mathbf{kv}}}^{\frac{1}{2}})$ . Thus the optimal rank- $k$  solution to  $\widetilde{\mathbf{W}}_{\mathbf{q},i}$  is:

$$\widetilde{\mathbf{W}}_{\mathbf{q},i} = \left(\mathbf{R}_{\mathbb{X}_{\mathbf{q}}\mathbb{X}_{\mathbf{q}}}^{\frac{1}{2}}\right)^{-1} \operatorname{SVD}_r \left(\mathbf{R}_{\mathbb{X}_{\mathbf{q}}\mathbb{X}_{\mathbf{q}}}^{\frac{1}{2}} \mathbf{W}_{\mathbf{q},i} \mathbf{R}_{\mathbb{X}_{\mathbf{kv}}\mathbb{X}_{\mathbf{kv}}}^{\frac{1}{2}}\right) \left(\mathbf{R}_{\mathbb{X}_{\mathbf{kv}}\mathbb{X}_{\mathbf{kv}}}^{\frac{1}{2}}\right)^{-1}. \quad (32)$$

□

## B.2 A<sup>3</sup>-OV

### B.2.1 Equivalent Objective

Similarly, we provide the derivation of the equivalent objective in Problem 2:

$$\begin{aligned} & \operatorname{argmin}_{\widetilde{\mathbf{W}}_{\text{vo},i}} \mathbb{E}_{\mathbf{p}_i \sim \mathbb{P}_i} \{ \|\mathbf{p}_i(\mathbf{W}_{\text{vo},i} - \widetilde{\mathbf{W}}_{\text{vo},i})\|_F^2 \} \quad \text{s.t.} \quad \operatorname{rank}(\widetilde{\mathbf{W}}_{\text{vo},i}) = r \\ & \Rightarrow \operatorname{argmin}_{\widetilde{\mathbf{W}}_{\text{vo},i}} \mathbb{E}_{\mathbf{p}_i \sim \mathbb{P}_i} \{ \|\mathbf{R}_{\mathbb{X}_{\mathbf{p}_i} \mathbb{X}_{\mathbf{p}_i}}^{\frac{1}{2}} (\mathbf{W}_{\text{vo},i} - \widetilde{\mathbf{W}}_{\text{vo},i})\|_F^2 \}. \end{aligned} \quad (33)$$

*Proof.* We begin with the right-hand side (RHS) of Equation (33). For clarity, we define some intermediate variables:

$$\mathbf{C} := [\mathbf{c}_1^T, \mathbf{c}_2^T, \dots, \mathbf{c}_{d_m}^T]^T = \mathbf{W}_{\text{vo},i} - \widetilde{\mathbf{W}}_{\text{vo},i}, \quad \mathbf{p}_i = [p_{i,1} \quad p_{i,2} \quad \dots \quad p_{i,d_m}] , \quad (34)$$

$$\begin{aligned} & \mathbb{E}_{\mathbf{p}_i \sim \mathbb{P}_i} \{ \|\mathbf{p}_i(\mathbf{W}_{\text{vo},i} - \widetilde{\mathbf{W}}_{\text{vo},i})\|_F^2 \} \\ &= \mathbb{E}_{\mathbf{p}_i \sim \mathbb{P}_i} \{ \left\| [p_{i,1} \quad p_{i,2} \quad \dots \quad p_{i,d_m}] [\mathbf{c}_1^T, \mathbf{c}_2^T, \dots, \mathbf{c}_{d_m}^T]^T \right\|_F^2 \} \\ &= \mathbb{E}_{\mathbf{p}_i \sim \mathbb{P}_i} \left\{ \left\| \left( \sum_j^{d_m} p_{i,j} \mathbf{c}_j \right) \right\|_F^2 \right\} \\ &= \mathbb{E}_{\mathbf{p}_i \sim \mathbb{P}_i} \left\{ \left\| \sum_j^{d_m} p_{i,j} \mathbf{c}_j \right\|_F^2 \right\} \\ &= \mathbb{E}_{\mathbf{p}_i \sim \mathbb{P}_i} \left\{ \left( \sum_j^{d_m} p_{i,j} \mathbf{c}_j \right) \left( \sum_j^{d_m} p_{i,j} \mathbf{c}_j \right)^T \right\} \\ &= \mathbb{E}_{\mathbf{p}_i \sim \mathbb{P}_i} \{ \mathbf{e}((\mathbf{p}^T \mathbf{p}) \odot (\mathbf{C} \mathbf{C}^T)) \mathbf{e}^T \} \\ &= \mathbb{E}_{\mathbf{p}_i \sim \mathbb{P}_i} \{ \operatorname{Tr}((\mathbf{p}^T \mathbf{p})(\mathbf{C} \mathbf{C}^T)) \} \\ &= \operatorname{Tr}(\mathbb{E}_{\mathbf{p}_i \sim \mathbb{P}_i} \{ \mathbf{p}^T \mathbf{p} \} (\mathbf{C} \mathbf{C}^T)) \\ &= \operatorname{Tr}(\mathbf{R}_{\mathbb{X}_{\mathbf{p}_i} \mathbb{X}_{\mathbf{p}_i}} \mathbf{C} \mathbf{C}^T) \\ &= \operatorname{Tr}(\mathbf{R}_{\mathbb{X}_{\mathbf{p}_i} \mathbb{X}_{\mathbf{p}_i}}^{\frac{1}{2}} \mathbf{C} \mathbf{C}^T (\mathbf{R}_{\mathbb{X}_{\mathbf{p}_i} \mathbb{X}_{\mathbf{p}_i}}^{\frac{1}{2}})^T) \\ &= \|\mathbf{R}_{\mathbb{X}_{\mathbf{p}_i} \mathbb{X}_{\mathbf{p}_i}}^{\frac{1}{2}} (\mathbf{W}_{\text{vo},i} - \widetilde{\mathbf{W}}_{\text{vo},i})\|_F^2 , \end{aligned} \quad (35)$$

where  $\mathbf{e} = [1, 1, \dots, 1]$  is a row vector of  $d_m$  ones. □

### B.2.2 Analytical Solution

Here we provide the proof of Theorem 3.

*Proof.* We continue with Equation 35:

$$\begin{aligned} & \operatorname{argmin}_{\widetilde{\mathbf{W}}_{\text{vo},i}} \mathbb{E}_{\mathbf{p}_i \sim \mathbb{P}_i} \{ \|\mathbf{p}_i(\mathbf{W}_{\text{vo},i} - \widetilde{\mathbf{W}}_{\text{vo},i})\|_F^2 \} \quad \text{s.t.} \quad \operatorname{rank}(\widetilde{\mathbf{W}}_{\text{vo},i}) = r \\ & \Rightarrow \operatorname{argmin}_{\widetilde{\mathbf{W}}_{\text{vo},i}} \|\mathbf{R}_{\mathbb{X}_{\mathbf{p}_i} \mathbb{X}_{\mathbf{p}_i}}^{\frac{1}{2}} (\mathbf{W}_{\text{vo},i} - \widetilde{\mathbf{W}}_{\text{vo},i})\|_F^2 . \end{aligned} \quad (36)$$

Note that multiplication by the invertible matrix  $\mathbf{R}_{\mathbb{X}_{\mathbf{p}_i} \mathbb{X}_{\mathbf{p}_i}}$  does not change the rank of the matrix  $\mathbf{W}_{\text{vo},i}$ . According to the Eckart-Young-Mirsky theorem [Eckart and Young, 1936b], the optimal rank  $r$  approximation to  $(\mathbf{R}_{\mathbb{X}_{\mathbf{p}_i} \mathbb{X}_{\mathbf{p}_i}}^{\frac{1}{2}} \mathbf{W}_{\text{vo},i})$  is the truncated SVD of  $(\mathbf{R}_{\mathbb{X}_{\mathbf{p}_i} \mathbb{X}_{\mathbf{p}_i}}^{\frac{1}{2}} \mathbf{W}_{\text{vo},i})$ :

$$(\mathbf{R}_{\mathbb{X}_{\mathbf{p}_i} \mathbb{X}_{\mathbf{p}_i}}^{\frac{1}{2}} \mathbf{W}_{\text{vo},i})_r = \mathbf{U}_{:,r} \boldsymbol{\Sigma}_{:r,:r} \mathbf{V}_{:r,:}^T , \quad (37)$$



where  $U\Sigma V^T = \text{SVD}\left(R_{\mathbb{X}_{\mathbf{p}_i} \mathbb{X}_{\mathbf{p}_i}}^{\frac{1}{2}} \mathbf{W}_{\text{vo},i}\right)$ . Thus the optimal rank- $k$  solution to  $\widetilde{\mathbf{W}}_{\text{vo},i}$  is:

$$\widetilde{\mathbf{W}}_{\text{vo},i} = \left(R_{\mathbb{X}_{\mathbf{p}_i} \mathbb{X}_{\mathbf{p}_i}}^{\frac{1}{2}}\right)^{-1} \text{SVD}_r\left(R_{\mathbb{X}_{\mathbf{p}_i} \mathbb{X}_{\mathbf{p}_i}}^{\frac{1}{2}} \mathbf{W}_{\text{vo},i}\right). \quad (38)$$

□

### B.2.3 Alternative Solution to A<sup>3</sup>-OV

Here we elaborate on the alternative solution to Problem 2 by directly minimizing  $\|\mathbf{o} - \widetilde{\mathbf{o}}\|_2^2$  through matrix stacking. With matrix stacking, we can write the overall attention output as two matrix multiplications:

$$\mathbf{o} = \sum_{i=1}^{h_q} \mathbf{o}_i = \sum_{i=1}^{h_q} \mathbf{p}_i \mathbf{W}_{\text{vo},i} = \begin{bmatrix} \mathbf{p}_1 & \mathbf{p}_2 & \cdots & \mathbf{p}_{h_q} \end{bmatrix} \begin{bmatrix} \mathbf{W}_{\text{vo},1} \\ \mathbf{W}_{\text{vo},2} \\ \vdots \\ \mathbf{W}_{\text{vo},h_q} \end{bmatrix} = \mathbf{p}_{\text{cat}} \mathbf{W}_{\text{vo,cat}}, \quad (39)$$

where  $\mathbf{p}_{\text{cat}} \in \mathbb{R}^{d_m d_{h_{kv}}}$ ,  $\mathbf{W}_{\text{vo,cat}} \in \mathbb{R}^{d_m d_{h_{kv}} \times d_m}$  denote the concatenated attention score weighted values and the fused value/output projection.

The overall term  $\mathbf{o}$  takes the form of a linear layer  $\mathbf{o} = \mathbf{p}_{\text{cat}} \mathbf{W}_{\text{vo,cat}}$ . If  $\widetilde{\mathbf{o}} = \mathbf{p}_{\text{cat}} \widetilde{\mathbf{W}}_{\text{vo,cat}}$  denotes the approximated  $\mathbf{o}$ , the optimal solution to  $\widetilde{\mathbf{W}}_{\text{vo,cat}}$  is already given by Equation (8).

**Problem 4** (Minimization of overall attention output error). Given a pretrained Transformer layer, the attention output of OV component  $\mathbf{o} = \mathbf{p}_{\text{cat}} \mathbf{W}_{\text{vo,cat}}$  and its approximated form  $\widetilde{\mathbf{o}} = \mathbf{p}_{\text{cat}} \widetilde{\mathbf{W}}_{\text{vo,cat}}$ , approximating the fused value/output projection by minimizing the output error is to minimize the following expectation:

$$\text{argmin}_{\widetilde{\mathbf{W}}_{\text{vo,cat}}} \mathbb{E}_{\mathbf{p}_{\text{cat}} \sim \mathbb{P}_{\text{cat}}} \{\|\mathbf{p}_{\text{cat}}(\mathbf{W}_{\text{vo,cat}} - \widetilde{\mathbf{W}}_{\text{vo,cat}})\|_F^2\} \quad \text{s.t.} \quad \text{rank}(\widetilde{\mathbf{W}}_{\text{vo,cat}}) = r. \quad (40)$$

**Theorem 5** (A<sup>3</sup>-OV-overall for MHA-NoPE). *The optimal solution to Problem 4 is*

$$\widetilde{\mathbf{W}}_{\text{vo,cat}} = \left(R_{\mathbb{X}_{\mathbf{p}_{\text{cat}}} \mathbb{X}_{\mathbf{p}_{\text{cat}}}}^{\frac{1}{2}}\right)^{-1} \text{SVD}_r\left(R_{\mathbb{X}_{\mathbf{p}_{\text{cat}}} \mathbb{X}_{\mathbf{p}_{\text{cat}}}}^{\frac{1}{2}} \mathbf{W}_{\text{vo,cat}}\right), \quad (41)$$

where  $R_{\mathbb{X}_{\mathbf{p}_{\text{cat}}} \mathbb{X}_{\mathbf{p}_{\text{cat}}}} := \mathbb{E}_{\mathbf{p}_{\text{cat}} \sim \mathbb{P}_{\text{cat}}}$  is the autocorrelation matrix respect to the input space of  $\mathbf{p}_{\text{cat}}$  and  $R_{\mathbb{X}_{\mathbf{p}_{\text{cat}}} \mathbb{X}_{\mathbf{p}_{\text{cat}}}}^{\frac{1}{2}}$  denotes its unique symmetric matrix square root.

Similar to QK component, in practice we assign

$$\mathbf{L}_{vO} := \left(R_{\mathbb{X}_{\mathbf{p}_{\text{cat}}} \mathbb{X}_{\mathbf{p}_{\text{cat}}}}^{\frac{1}{2}}\right)^{-1} \mathbf{U}_{:,k}, \quad \mathbf{R}_{vO} := \Sigma_{:,k,:k} \mathbf{V}_{:,k,:}^T \left(R_{\mathbb{X}_{\mathbf{p}_{\text{cat}}} \mathbb{X}_{\mathbf{p}_{\text{cat}}}}^{\frac{1}{2}}\right)^{-1},$$

to get the approximated fused value/output weights with two low-rank matrices. In terms of attention head,  $\mathbf{L}_{vO}$  can be viewed as concatenating all value heads with head dimension of  $r$  together, and  $\mathbf{R}_{vO}$  can be viewed as a shared output head across the values:

$$\mathbf{L}_{vO} := \begin{bmatrix} \mathbf{L}_{v,1} \\ \mathbf{L}_{v,2} \\ \vdots \\ \mathbf{L}_{v,h_q} \end{bmatrix}, \quad \mathbf{R}_{vO} = \mathbf{R}_O,$$

where  $\mathbf{L}_{v,i} \in \mathbb{R}^{d_m \times r}$  and  $\mathbf{R}_O \in \mathbb{R}^{r \times d_m}$ . Attention output can then be computed as follows:

$$\mathbf{o} = \sum_{i=1}^{h_q} \mathbf{p}_i \mathbf{X}_{kv} \mathbf{L}_{v,i} \mathbf{R}_O. \quad (42)$$

Although this solution can theoretically save more parameters than minimizing the per-head attention output loss under the same model performance, it requires significantly more KV-cache storage, even exceeding that of the uncompressed model. This is because the shared rank  $r$  across all heads typically needs to be larger than  $d_{\text{vo}}$  of one head to maintain competitive performance. As a result, the KV-cache size increases by a factor of  $\frac{r}{d_{\text{vo}}}$  compared to uncompressed models.

### B.3 A<sup>3</sup>-MLP

#### B.3.1 Equivalent Objective

Here we provide the derivation of Lemma 4 in Problem 3:

$$\begin{aligned} & \operatorname{argmin}_{U=\operatorname{diag}(u_1, u_2, \dots, u_{d_{\text{inter}}})} \mathbb{E}_{\mathbf{x}_d \sim \mathbb{X}_d} \{ \|\mathbf{x}_d U \mathbf{W}_d - \mathbf{x}_d \mathbf{W}_d\|_2^2 \} \quad \text{s.t.} \quad \operatorname{rank}(U) = r \\ & \Rightarrow \operatorname{argmin}_{U=\operatorname{diag}(u_1, u_2, \dots, u_{d_{\text{inter}}})} \mathbb{E}_{\mathbf{p}_i \sim \mathbb{P}_i} \{ \|\mathbf{R}_{\mathbb{X}_d \mathbb{X}_d}^{\frac{1}{2}} U \mathbf{W}_d - \mathbf{R}_{\mathbb{X}_d \mathbb{X}_d}^{\frac{1}{2}} \mathbf{W}_d\|_F^2 \} . \end{aligned} \quad (43)$$

*Proof.* We begin with the right-hand side (RHS) of Equation (43). For clarity, we define some intermediate variables:

$$\mathbf{V} := (U \mathbf{W}_{\text{down}} - \mathbf{W}_{\text{down}}) = [\mathbf{v}_1^T, \mathbf{v}_2^T, \dots, \mathbf{v}_{d_{\text{inter}}}^T]^T, \quad \mathbf{x}_{\text{down}} = [x_1 \quad x_2 \quad \dots \quad x_{d_{\text{inter}}}] . \quad (44)$$

We continue by substituting Equation (44) to RHS of Equation (43):

$$\begin{aligned} & \mathbb{E}_{\mathbf{x}_d \sim \mathbb{X}_d} \{ \|\mathbf{x}_d U \mathbf{W}_d - \mathbf{x}_d \mathbf{W}_d\|_2^2 \} \\ &= \mathbb{E}_{\mathbf{x}_d \sim \mathbb{X}_d} \{ \|\mathbf{x}_d \mathbf{V}\|_2^2 \} \\ &= \mathbb{E}_{\mathbf{x}_d \sim \mathbb{X}_d} \left\{ \left\| \sum_i^{d_{\text{inter}}} x_i \mathbf{v}_i \right\|_2^2 \right\} \\ &= \mathbb{E}_{\mathbf{x}_d \sim \mathbb{X}_d} \left\{ \left( \sum_i^{d_{\text{inter}}} x_i \mathbf{v}_i \right) \left( \sum_i^{d_{\text{inter}}} x_i \mathbf{v}_i \right)^T \right\} \\ &= \mathbb{E}_{\mathbf{x}_d \sim \mathbb{X}_d} \left\{ \left( \sum_i^{d_{\text{inter}}} \sum_j^{d_{\text{inter}}} x_i x_j \mathbf{v}_i \mathbf{v}_j^T \right) \right\} \\ &= \mathbb{E}_{\mathbf{x}_d \sim \mathbb{X}_d} \{ \mathbf{e}((\mathbf{x}_d^T \mathbf{x}_d) \odot (\mathbf{V} \mathbf{V}^T)) \mathbf{e}^T \} \\ &= \mathbb{E}_{\mathbf{x}_d \sim \mathbb{X}_d} \{ \operatorname{Tr}((\mathbf{x}_d^T \mathbf{x}_d) (\mathbf{V} \mathbf{V}^T)) \} \\ &= \operatorname{Tr}(\mathbb{E}_{\mathbf{x}_d \sim \mathbb{X}_d} \{ \mathbf{x}_d^T \mathbf{x}_d \} (\mathbf{V} \mathbf{V}^T)) \\ &= \operatorname{Tr}(\mathbf{R}_{\mathbb{X}_d \mathbb{X}_d} \mathbf{V} \mathbf{V}^T) \\ &= \operatorname{Tr}(\mathbf{R}_{\mathbb{X}_d \mathbb{X}_d}^{\frac{1}{2}} \mathbf{V} \mathbf{V}^T (\mathbf{R}_{\mathbb{X}_d \mathbb{X}_d}^{\frac{1}{2}})^T) \\ &= \|\mathbf{R}_{\mathbb{X}_d \mathbb{X}_d}^{\frac{1}{2}} \mathbf{V}\|_F^2 \\ &= \|\mathbf{R}_{\mathbb{X}_d \mathbb{X}_d}^{\frac{1}{2}} U \mathbf{W}_d - \mathbf{R}_{\mathbb{X}_d \mathbb{X}_d}^{\frac{1}{2}} \mathbf{W}_d\|_F^2 . \end{aligned} \quad (45)$$

□

### B.4 Extending A<sup>3</sup> for GQA

Similar to GQA's QK Component, we can apply joint SVD to the OV component. The concatenation is done along the second dimension:

$$\operatorname{SVD} \left( \left[ \mathbf{R}_{\mathbb{X}_{kv} \mathbb{X}_{kv}}^{\frac{1}{2}} \widetilde{\mathbf{W}}_{\text{vo},1} \quad \dots \quad \mathbf{R}_{\mathbb{X}_{kv} \mathbb{X}_{kv}}^{\frac{1}{2}} \widetilde{\mathbf{W}}_{\text{vo},g} \right] \right) = U \Sigma V^T . \quad (46)$$

Then we make the assignment below to build the shared value head weights  $\widetilde{\mathbf{W}}_{\text{v, shared}}$  and the  $i$ -th approximated output head weights  $\widetilde{\mathbf{W}}_{0,i}$  for this group.

$$\widetilde{\mathbf{W}}_{0,i} := V_{:, i d_m : (i+1) d_m}^T \left( \mathbf{R}_{\mathbb{X}_{kv} \mathbb{X}_{kv}}^{\frac{1}{2}} \right)^{-1}, \quad \widetilde{\mathbf{W}}_{\text{v, shared}} := U_{:, :r \Sigma : r, :r} . \quad (47)$$

Note that in Equation (46) we use  $\mathbf{R}_{\mathbb{X}_{kv} \mathbb{X}_{kv}}$  instead of  $\mathbf{R}_{\mathbb{X}_{p_i} \mathbb{X}_{p_i}}$ , because  $\mathbf{R}_{\mathbb{X}_{p_i} \mathbb{X}_{p_i}}$  is head-specific, which prevents us from building a shared  $\widetilde{\mathbf{W}}_{\text{v, shared}}$  for all heads in the same GQA group. We name these two methods A<sup>3</sup>-QK-CR and A<sup>3</sup>-OV-CR for GQA's QK and OV components respectively.

## B.5 Extending $A^3$ for RoPE

Instead of sorting by the product of  $l_2$ -norm,  $\lambda_i = \|\mathbf{L}_{:,i}\|_2^2 \cdot \|\mathbf{R}_{i,:}\|_2^2$ , for  $i = 0, 1, \dots, d_{\text{qk}} - 1$ , we sort by the sum of  $\lambda_i$  of adjacent pairs:

$$\lambda_{2i} = \|\mathbf{L}_{:,2i}\|_2^2 \cdot \|\mathbf{R}_{2i,:}\|_2^2 + \|\mathbf{L}_{:,2i+1}\|_2^2 \cdot \|\mathbf{R}_{2i+1,:}\|_2^2 \quad \text{for } i = 0, 1, \dots, \frac{d_{\text{qk}}}{2} - 1. \quad (48)$$

This will drop pairs of less important columns in  $\mathbf{L}$  and rows in  $\mathbf{R}$ , as well as the corresponding pairs of RoPE frequencies. This requires a frequency index array for each QK pair, and indexing the RoPE constants at runtime. Usually the head dimension  $d_{\text{qk}}$  is 64 or 128, so the RoPE frequency indices can be saved in a compact INT8 array. However, to achieve high throughput/low latency, a custom kernel is needed to fuse indexing and rotation together, which is out of the scope of this paper.

This RoPE extension can be combined with the GQA extension, which means the sorting in Equation (48) is done on the concatenated  $\mathbf{L}$  and  $\mathbf{R}$  matrices in Equation (22).

## C Detailed Experiment Setup

**Calibration** We concatenate the texts in SlimPajama and randomly sample 128 sequences of 2048 tokens for calibration. We only calibrate on WikiText-2 for Table 7. SlimPajama is a pretraining dataset of high-quality corpus, better capturing the statistics of auto-correlation than WikiText2. We calibrate the auto-correlation matrix using BF16 models, but accumulate the outer product in FP64.

**Approximation** Since the autocorrelation matrix is symmetric and positive semi-definite, we used SVD to calculate its inverse and matrix square root, which improves the numerical stability. For GQA models, we also use `torch.svd_lowrank` instead of `torch.linalg.svd` for faster solving.

**Downstream evaluation** We use 0-shot prompting for BoolQ and OpenBookQA, 5-shot for Winogrande, GSM8K, and MMLU, 25-shot for ARC-c. Other evaluation parameters are kept as the default provided by `lm-eval-harness`.

**Sever specs** We run all the experiments on two GPU boxes, one with two NVIDIA H100s, and the other with 8 NVIDIA A100s. In total, we spent around 1200 GPU hours on running  $A^3$ , and 800 hours on baselines. Specifically, for MHA models, most of the GPU hours were spent on calibration and VO solving. For GQA models, `torch.svd_lowrank` speeds up the VO solving, with most of the GPU hours on calibration and FFN solving. For the ASVD baseline, most of the GPU hours were on the mixed-rank search, while other baselines took most of the time on calibration and approximation. Since all the calibration, approximation, and evaluation were run on GPUs, our experiments were not bottlenecked by CPUs.

## D Discussion

**Quantization compatibility** Here we show that  $A^3$  can be combined together with quantization. Figure 6 presents the perplexity of quantized LLaMA-3.1-8B with HQQ 4-bit quantization, before and after applying  $A^3$ . The small amount of extra model performance degradation caused by  $A^3$  indicates its orthogonality to quantization.

**Mixed-rank allocation** SVD-LLM v2 [Wang et al., 2025] and ASVD [Yuan et al., 2023] have demonstrated that different layers exhibit varying sensitivity to rank reduction. Here we show that  $A^3$  can also benefit from mixed-rank allocation, achieving performance gain with minimal effort. Specifically, we conduct a simple search over rank allocations for each decoder layer in LLaMA-7b. As shown in Table 5,  $A^3$ -mixed outperforms both the uniform  $A^3$  and other mixed-rank approaches.

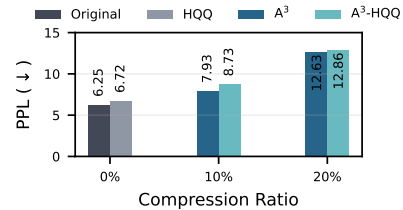


Figure 6: A comparison of perplexity ( $\downarrow$ ) on WikiText-2 using quantization (HQQ, 4 bits) for both the original and  $A^3$ -applied LLaMA-3.1-8B.

**Limitation of CUR decomposition** One limitation of  $A^3$  is its reliance on CUR decomposition for RoPE-based attention and MLP, which does not guarantee an optimal solution like SVD. When targeting a small compression ratio (*e.g.*, CRatio=10%), CUR decomposition provides a good trade-off between performance and compression. As the compression ratio increases, its performance degrades much faster than SVD and is eventually surpassed by SVD-based approaches. However, we argue that even for SVD-based approaches, the model performance under a compression ratio larger than 10% is already very poor. For example, the C4 perplexity of LLaMA-3.1-70B with CRatio=20% is 13.77 for SVD-LLM, which is even higher than the original LLaMA-3.1-8B. A retraining is needed in this case, but is out of the scope of this paper.

**Choice of calibration datasets** We compared the model performance when calibrating on SlimPajama and WikiText-2. We find calibrating on SlimPajama gives closer perplexities on Wikitext-2 and C4, regardless of the compression level (Appendix Table 6). However, calibrating on WikiText-2 has a widening perplexity gap between WikiText-2 and C4 as the compression ratio increased, especially for SVD-LLM, which potentially indicates overfitting. We hypothesize that this may contribute to cases where SVD-LLM appears to perform better on particular downstream tasks, like Winogrande, in Table 2. To validate this, we used a more diverse calibration set with samples from SlimPajama and PTB in Table 7. The results show that with this mixture of calibration sets,  $A^3$  achieves a higher accuracy than SVD-LLM on Winogrande.

Table 5: A comparison of perplexity ( $\downarrow$ ) on WikiText-2 and C4 of LLaMA-7B under 20% mixed-rank compression rate.

Method	WikiText-2	C4
Original	5.68	7.65
$A^3$	7.21	10.01
SVD-LLM v2	10.53	13.00
ASVD	10.45	13.1
$A^3$ -mix	<b>7.11</b>	<b>9.86</b>

Table 6: Performance of LLaMA-7b compressed by SVD-LLM and  $A^3$  under different compression ratio using calibration data sampled from SlimPajama (our setting) and WikiText-2 datasets. The performance are reported by the average and difference in perplexity ( $\downarrow$ ) of Wikitext-2 and C4 datasets.

Method	10%		20%		40%	
	Avg	$ \Delta $	Avg	$ \Delta $	Avg	$ \Delta $
SVD-LLM (SlimPajama)	9.50	2.54	9.50	2.54	30.84	1.00
$A^3$ (SlimPajama)	7.24	2.24	8.52	2.79	25.22	9.83
SVD-LLM (WikiText-2)	9.62	5.07	11.89	7.90	44.58	61.69
$A^3$ (WikiText-2)	7.24	2.25	8.50	3.68	12.82	18.95

Table 7: Performance evaluation of LLaMA-3.1-8b (20% compression) using SVD-LLM and  $A^3$  with two calibration datasets: SlimPajama and a 50/50 SlimPajama-PTB mixture. Metrics include perplexity ( $\downarrow$ ) of Wikitext-2, C4 and slimPajama, and accuracy ( $\uparrow$ ) of BoolQ, Winogrande, ARC-c (with their average).

Method	WikiText-2	C4	SlimPajama	BoolQ	Winogrande	ARC-c	Avg.
SVD-LLM (SlimPajama)	42.28	33.6	27.44	0.6948	0.644	0.2534	0.5307
$A^3$ (SlimPajama)	11.36	17.87	13.58	0.6823	0.6417	0.3345	0.5528
SVD-LLM (SlimPajama+PTB)	36.76	36.62	31.79	0.7349	0.6717	0.2671	0.5579
$A^3$ (SlimPajama+PTB)	11.47	18.57	14.30	0.7220	0.6938	0.3524	0.5894